

Danger peptide receptor signaling in plants ensures basal immunity upon pathogen-induced depletion of BAK1

Kohji Yamada^{1,2}, Misuzu Yamashita-Yamada^{1,†,‡}, Taishi Hirase^{3,‡}, Tadashi Fujiwara³, Kenichi Tsuda¹, Kei Hiruma³ & Yusuke Saijo^{1,3,4,*}

Abstract

Pathogens infect a host by suppressing defense responses induced upon recognition of microbe-associated molecular patterns (MAMPs). Despite this suppression, MAMP receptors mediate basal resistance to limit host susceptibility, via a process that is poorly understood. The *Arabidopsis* leucine-rich repeat (LRR) receptor kinase BAK1 associates and functions with different cell surface LRR receptors for a wide range of ligands, including MAMPs. We report that BAK1 depletion is linked to defense activation through the endogenous PROPEP peptides (Pep epitopes) and their LRR receptor kinases PEPR1/PEPR2, despite critical defects in MAMP signaling. In *bak1*-knockout plants, PEPR elicitation results in extensive cell death and the prioritization of salicylate-based defenses over jasmonate-based defenses, in addition to elevated proligand and receptor accumulation. BAK1 disruption stimulates the release of PROPEP3, produced in response to Pep application and during pathogen challenge, and renders PEPRs necessary for basal resistance. These findings are biologically relevant, since specific BAK1 depletion coincides with PEPR-dependent resistance to the fungal pathogen *Colletotrichum higginsianum*. Thus, the PEPR pathway ensures basal resistance when MAMP-triggered defenses are compromised by BAK1 depletion.

Keywords *Arabidopsis*; BAK1; DAMP; PEPR; plant immunity

Subject Categories Plant Biology; Microbiology, Virology & Host Pathogen Interaction; Immunology

DOI 10.15252/embj.201591807 | Received 15 April 2015 | Revised 15 October 2015 | Accepted 20 October 2015 | Published online 16 November 2015

The EMBO Journal (2016) 35: 46–61

See also: **D Tang & J-M Zhou** (January 2016)

Introduction

Innate immunity based on a limited set of germ line-encoded receptors is fundamental for both plants and animals to recognize and respond to diverse microbes (Ronald & Beutler, 2010). Plants rely solely on innate immunity, which involves two tiers of functionally interlinked immune responses. The first is mediated by cell surface-localized pattern recognition receptors (PRRs) that sense molecular signatures typical of microbes, termed microbe-associated molecular patterns (MAMPs), including bacterial flagellin, elongation factor (EF)-Tu, peptidoglycans, and fungal chitin (Boller & Felix, 2009; Macho & Zipfel, 2014). MAMP-triggered immunity (MTI) is typically insufficient to prevent infection by host-adapted pathogens that employ an array of virulence effectors to subvert PRR-mediated defenses. However, the second tier of plant immunity is triggered when these effectors are recognized. Effector-triggered immunity (ETI) leads to a robust and high-amplitude activation of immune responses that terminate pathogen growth, which is often accompanied by localized cell death. A large overlap in the defense outputs and signaling components leads to the notion that ETI is a magnified form of MTI (Jones & Dangl, 2006; Cui *et al.*, 2015).

ETI is often induced upon recognition of effector-mediated modifications of a host target (Cui *et al.*, 2015). Animal studies have also described pathogen effectors that elicit immune responses to protect the host (Stuart *et al.*, 2013). Defense activation upon sensing pathogen effectors seems to represent a key principle in both plant immunity and animal immunity.

In plants, substantial defenses are activated when susceptible hosts are challenged with virulent pathogens, and thereby limit host susceptibility. This response, known as basal resistance (Jones & Dangl, 2006), seems not to require the recognition of a specific pathogen effector, but is often enhanced when plants deficient in MAMP responses are exposed to pathogen effectors (Laluk *et al.*, 2011; Li *et al.*, 2014). These observations imply a link between basal resistance and pathogen effector actions. On the other hand, loss of

1 Department of Plant-Microbe Interactions, Max Planck Institute for Plant Breeding Research, Cologne, Germany

2 Graduate School of Agriculture, Kyoto University, Kyoto, Japan

3 Graduate School of Biological Sciences, Nara Institute of Science and Technology, Ikoma, Japan

4 JST, PRESTO, Kawaguchi, Japan

*Corresponding author. Tel: +81 743 72 5690; E-mail: saijo@bs.naist.jp

†Present address: Faculty of Life and Environmental Sciences, University of Tsukuba, Tsukuba, Japan

‡These authors contributed equally to this work

individual MAMP receptors increases host susceptibility to virulent pathogens having a complete effector assembly (Zipfel *et al*, 2004, 2006; Willmann *et al*, 2011), indicating a critical role for MAMP recognition in basal resistance. However, it remains poorly understood how MAMP receptors mediate host resistance despite effector-mediated suppression of MTI signaling.

In *Arabidopsis*, the leucine-rich repeat (LRR) receptor kinases (RKs) FLS2 and EFR recognize the bacterial MAMPs flagellin (flg22 epitope) and EF-Tu (elf18 epitope), respectively, and induce antibacterial immunity (Zipfel *et al*, 2004, 2006). Immediately after ligand binding, FLS2/EFR physically associate with the LRR-RK coreceptor BAK1, thereby offering a platform for defense signaling (Chinchilla *et al*, 2007; Heese *et al*, 2007; Sun *et al*, 2013). The FLS2/EFR-BAK1 complexes mediate phosphorylation of the receptor-like cytoplasmic kinases (RLCKs) BIK1 and related PBL proteins, which in turn dissociate from the receptor complexes to regulate downstream signaling (Lu *et al*, 2010; Zhang *et al*, 2010; Liu *et al*, 2013; Lin *et al*, 2014). These events are followed by a stereotypic set of cellular responses, including a rapid burst of Ca²⁺ and reactive oxygen species (ROS), activation of Ca²⁺-dependent protein kinases (CDPKs) and mitogen-activated protein kinases (MAPKs), cell wall remodeling, production of the phytohormones ethylene (ET) and salicylate (SA), and extensive transcriptional reprogramming (Boller & Felix, 2009; Macho & Zipfel, 2014).

Fine control of MAMP signaling is in part achieved through negative regulation within or in proximity to the PRR-BAK1 complexes. For instance, the LRR-RK BIR2 sequesters BAK1 from ligand-unbound FLS2 to avoid precocious signal activation (Halter *et al*, 2014). The BAK1-associated E3 ubiquitin ligases PUB12/PUB13 are recruited to the ligand-induced FLS2-BAK1 complex for ubiquitination and proteasomal degradation of the receptor (Lu *et al*, 2011). A ligand-induced decrease in FLS2 accumulation, apparently in association with receptor internalization, results in transient desensitization to flg22 before subsequent replenishment of the receptor (Robatzek *et al*, 2006; Smith *et al*, 2014). A subclass of protein phosphatase 2A dephosphorylates BAK1 to attenuate FLS2 signaling (Segonzac *et al*, 2014). However, it is less clear whether and how relief of negative regulation is linked to basal resistance during pathogen challenge.

MAMP signaling induces a subset of the soluble pro-peptide (PROPEP) family (carrying an immunogenic Pep epitope in their C termini) and then involves the LRR-RK Pep receptors PEPR1/PEPR2 (Huffaker *et al*, 2006; Yamaguchi *et al*, 2006, 2010; Krol *et al*, 2010; Ma *et al*, 2012; Tintor *et al*, 2013). The lack of N-terminal signal sequences for canonical secretion led to a model in which PROPEP-derived elicitors provide danger-associated molecular patterns (DAMPs) following their release upon membrane disintegration (Yamaguchi & Huffaker, 2011). Pep perception by PEPRs leads to MTI-hallmark outputs, largely through the aforementioned scheme of MTI signaling (Yamaguchi & Huffaker, 2011; Liu *et al*, 2013). The PEPR pathway contributes to co-activation of SA and jasmonate (JA)/ET defenses (Ross *et al*, 2014) and to propagation of MAMP-triggered defense signaling (Ma *et al*, 2012; Flury *et al*, 2013; Tintor *et al*, 2013; Ross *et al*, 2014). These findings point to the importance of functional interactions between the FLS2/EFR and PEPR pathways as a critical step in MTI. However, despite increasing insight into the individual PRR pathways, the mechanisms underlying their functional interactions remain poorly understood.

Of note, FLS2, EFR and PEPRs all function with BAK1 in signal initiation. It remains to be determined whether BAK1 provides a node of functional convergence or is simply a common component in separate PRR pathways. Nevertheless, either scenario predicts that MTI will be vulnerable to pathogen assaults on BAK1. Indeed, BAK1 is a recurrent target in different plant hosts for structurally and functionally unrelated virulence-promoting effectors (Xin & He, 2013; Macho & Zipfel, 2015). However, *bak1*-knockout (KO) plants display almost intact or even enhanced post-invasion resistance against (hemi)biotrophic pathogens (Kemmerling *et al*, 2007), despite critical defects in a major branch of MTI signaling (Liebrand *et al*, 2014).

In addition to PRR signaling, BAK1 positively regulates brassinosteroid (BR) signaling and negatively regulates cell death (Liebrand *et al*, 2014). BAK1 acts as a co-receptor for the LRR-RK BR receptor BRI1 (Nam & Li, 2002; Li *et al*, 2002). BR signaling and MTI signaling antagonize each other (Albrecht *et al*, 2012; Belkadir *et al*, 2012; Lin *et al*, 2013), but BAK1 is not rate-limiting between the two pathways (Albrecht *et al*, 2012). In cell death suppression, BAK1 acts together with the LRR-RK BIR1 and the membrane-associated copain-like BONZAI proteins BON1-BON3 (He *et al*, 2007; Kemmerling *et al*, 2007; Wang *et al*, 2011). Accordingly, *bak1*-KO plants exhibit enhanced cell death upon pathogen challenge, which is further enhanced by the loss of BKK1, the closest homolog of BAK1 (He *et al*, 2007; Kemmerling *et al*, 2007). Both *bir1* and *bon* mutant plants display spontaneous cell death that is partially suppressed at high temperatures and by the loss of the lipase-like proteins EDS1/PAD4 or the nucleotide-binding LRR receptor (NLR) SNC1 (Yang *et al*, 2006; Gao *et al*, 2009). These findings suggest a link between cell death and resistance in *bak1*-KO plants, which remains to be explored.

Here, we show that the loss of BAK1 sensitizes PEPR signaling toward cell death and results in reprogramming of PEPR-mediated defense outputs in favor of SA-related resistance. This is accompanied by increased extracellular release of PROPEP3 upon pathogen challenge. Notably, selective BAK1 depletion occurs during challenge with the fungal hemibiotrophic pathogen *Colletotrichum higginsianum* (Ch) and coincides with PEPR-dependent fungal resistance. Our findings indicate a critical role for PEPR-mediated DAMP signaling, which is stimulated and rewired when BAK1 is depleted, in plant immunity.

Results

Loss of BAK1 sensitizes PEPR-mediated signaling toward cell death

Pursuing a molecular link between MAMP and PEPR pathways, we investigated a role of BAK1 in PEPR signaling. With transgenic plants expressing a functional PEPR1-Flag fusion in the *pepr1 pepr2* background (Fig EV1A), co-immunoprecipitation (coIP) analyses confirmed ligand-induced association of PEPR1-Flag and BAK1 (Fig EV1B), as previously deduced (Schulze *et al*, 2010).

Unexpectedly, however, Pep2-induced growth inhibition was greatly enhanced in *bak1-3* and *bak1-4* KO plants compared to the wild type (WT) (Figs 1A and EV2A). This phenotype was rescued by the introduction of a genomic BAK1 clone (Fig EV2B) and abolished in *bak1 pepr1 pepr2* plants (Figs 1A and EV2A), confirming that Pep sensitization upon BAK1 disruption occurs through PEPRs. Of the

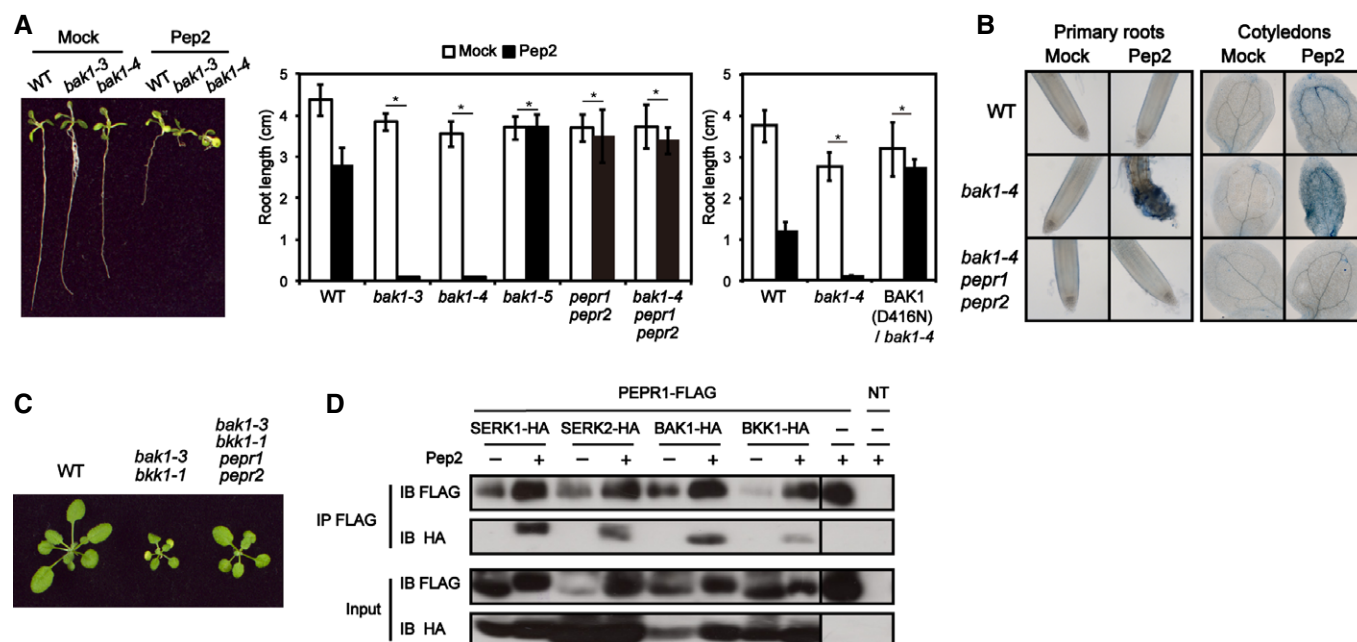


Figure 1. BAK1 disruption sensitizes PEPR signaling toward cell death.

A, B Root length (averages \pm SD, $n \geq 15$) (A) and cell death staining of cotyledons and primary root tips (B) of *Arabidopsis* seedlings that were exposed to 100 nM Pep2 for 7 days, 2 days after germination. BAK1 (D416N) is a kinase-dead variant. * $P < 0.05$ in two-tailed tests compared to the differences (\pm Pep2) from the corresponding values of WT plants.

C Overview of 3-week-old plants.

D Pep2 induces PEPR1-FLAG association with SERK1-, SERK2-, BKK1-, and BAK1-HA in *N. benthamiana*. Experiments were repeated at least three times, with the same conclusions. IP and IB denote immunoprecipitation and immunoblotting with the indicated antibodies, respectively. NT indicates non-transformed plants.

Source data are available online for this figure.

BAK1-related SERK family members, single disruption of *BAK1* specifically enhanced Pep2-induced growth inhibition (Fig EV2C), correlated with enhanced cell death (He *et al.*, 2007; Kemmerling *et al.*, 2007). Indeed, cell death staining revealed that Pep2, but not flg22, induced extensive cell death in the roots and cotyledons of *bak1-4* plants, in a manner dependent on PEPRs (Figs 1B and EV3A). This demonstrates that PEPR-mediated pro-death signaling is sensitized upon *BAK1* disruption. Moreover, loss of PEPRs substantially suppressed the dwarfism of *bak1 bkk1* plants (Fig 1C), suggesting a contribution of endogenous PROPEP-PEPR signaling to cell death in the mutant. We thus conclude that PEPRs mediate one of the pro-death pathways that are suppressed by BAK1/BKK1.

To assess the specificity of the *bak1* effects, we tested Pep2-induced growth inhibition in *lsd1c* plants, which display runaway cell death via EDS1 (Rustérucci *et al.*, 2001). In contrast to *bak1* plants, *lsd1* plants retained WT-like Pep2 sensitivity (Fig EV3B). *EDS1* disruption did not affect Pep2-induced growth arrest in *bak1* plants (Fig EV3C). These results suggest that PEPR-mediated pro-death signaling occurs independently of EDS1 and is specifically sensitized upon BAK1 disruption.

Enhanced cell death in *bak1* plants was previously uncoupled from BR signaling (He *et al.*, 2007; Kemmerling *et al.*, 2007). Consistent with this, neither the reduction nor the sensitization of BR signaling in the presence of the *bri1-301* allele (Nam & Li, 2002) or BES1-D (Albrecht *et al.*, 2008), respectively, influenced the *bak1* effects on Pep2-induced growth inhibition (Fig EV2D and E). Our

results thus rule out antagonism between BR and PRR signaling as the cause for the sensitization of Pep-induced cell death.

Disruption, but not catalytic inactivation, of BAK1 sensitizes PEPR signaling

To determine whether loss of BAK1 accumulation or kinase activity sensitizes PEPR signaling, we characterized the previously described *bak1* alleles (Schwessinger *et al.*, 2011; Ranf *et al.*, 2012). Pep2-induced root growth inhibition was enhanced in the tested *bak1*-null alleles relative to the corresponding WT controls, while, in contrast, that in the *bak1* alleles with a point substitution in the kinase domain, including a kinase-dead variant, was suppressed (Figs 1A and EV3E and F). In the hypoactive *bak1-5* allele (Schwessinger *et al.*, 2011), Pep-induced growth inhibition and MAPK activation were almost abolished (Figs 1A and EV1C). These results are consistent with the established view that BAK1 positively regulates PEPR signaling (Roux *et al.*, 2011). However, in contrast to catalytic inactivation of BAK1, our findings reveal that BAK1 depletion leads to the sensitization of PEPR-mediated pro-death signaling.

It is conceivable that another SERK member compensates for the absence of BAK1 in PEPR signaling but is virtually, if not completely, blocked in the presence of a kinase-inactive BAK1 variant. This model also explains the retention of PEPR function leading to growth inhibition in *bak1 bkk1* plants (Fig 1C). We thus tested pairwise associations between PEPR1 and SERK members by coIP

analyses in *Nicotiana benthamiana* leaves, following *Agrobacterium*-mediated co-expression of PEPR1-FLAG with individual SERK-HA proteins. In contrast to the preferential FLS2-BAK1 association (Roux *et al*, 2011), PEPR1-FLAG associated with the four tested SERK members in response to Pep2 (Fig 1D). Therefore, promiscuous employment of SERK members seems to underlie the tolerance of PEPR signaling to BAK1/BKK1 disruption.

PEPR signaling strictly requires BIK1 and PBL1

flg22, elf18 and Pep1 commonly induce phosphorylation of BIK1 and MAPKs, downstream of cognate PRR-BAK1 complexes (Lu *et al*, 2010; Zhang *et al*, 2010; Liu *et al*, 2013). PEPR1 directly phosphorylates BIK1, whereas FLS2 relies on BAK1 for BIK1 phosphorylation (Lu *et al*, 2010; Liu *et al*, 2013). Consistent with this, BIK1 phosphorylation and MAPK activation in response to Pep2 remain largely unaffected in *bak1*-KO plants, while those in response to flg22 were significantly reduced (Figs 2A and EV1C). By contrast, Pep responsiveness requires BIK1 and the closely related PBL1 (Liu *et al*, 2013). We verified that Pep2-induced MAPK activation and growth inhibition were reduced in *bak1 bik1 pbl1* plants (Fig 2B and C), demonstrating that the authentic PEPR-SERK-RLCK module mediates sensitized Pep responses in the absence of BAK1.

Reprogramming of the PEPR-regulated transcriptome upon BAK1 disruption

To elucidate the *bak1* effects on PEPR-regulated outputs, we performed a genome-wide microarray analysis for WT and *bak1-3* seedlings exposed to Pep2. The loss of BAK1 had a larger effect on Pep2-regulated expression profiles at 10 h than at 2 h (Fig 3A). Cross-referencing Pep2-responsive genes in *bak1* plants at 10 h with genes responsive to SA, methyl-JA and ET revealed an overrepresentation of SA- or JA-inducible genes among the Pep2 up- or down-regulated genes, respectively (Fig 3B; Table EV1). qRT-PCR analyses confirmed that Pep2 induction of SA-related and -unrelated defense markers, *PR1* and *NHL10*, respectively, was enhanced, while in contrast that of a JA/ET marker, *PDF1.2a*, was suppressed in *bak1*-KO plants (Fig 3C and D). BIK1/PBL1 were again required for enhanced Pep2 induction of *PR1* and *NHL10* in *bak1* plants (Fig 3D), indicating that the authentic PEPR-BIK1/PBL1 signaling is rewired

upon *BAK1* disruption. Together, our results suggest that BAK1 disruption leads to the prioritized activation of these SA-related and -unrelated defenses at the cost of the JA-dependent defenses.

Of particular note, although SID2-mediated SA biosynthesis (Wildermuth *et al*, 2001) was required for *PR1* induction in response to Pep2, it was dispensable for cell death, growth arrest, *NHL10* induction, and suppression of *PDF1.2a* induction in *bak1*-KO plants (Figs 3C and EV3D). These results point to the SA independence of pro-death signaling and of suppressing JA/ET defense induction via PEPRs upon *BAK1* disruption.

Loss of BAK1 reinforces the PEPR pathway at both the prolignand and receptor levels

PEPR-mediated *PROPEP2*/*PROPEP3* activation is thought to provide positive feedback for defense signal amplification (Yamaguchi & Huffaker, 2011). Pep2-induced *PROPEP2*/*PROPEP3* activation was enhanced in *bak1*-KO plants (Fig 4A). With anti-GFP and anti-*PROPEP3* antibodies (raised against both N- and C-terminal fragments of *PROPEP3*; Ross *et al*, 2014), we traced Pep2 induction of a functional *PROPEP3*-Venus fusion protein, driven by the native DNA regulatory sequences (Ross *et al*, 2014). To determine whether *PROPEP3*-Venus is released from the cell, we examined an extracellular protein fraction recovered from the surrounding liquid medium. Both antibodies detected a specific signal that is nearly of the predicted full-length size (~10.4 + 27 kDa) in both *in planta* and extracellular fractions (Fig 4B). The *PROPEP3*-Venus form was produced and released into the extracellular space in response to Pep2, to a greater degree in *bak1-4* plants compared to WT plants (Fig 4B). Although differences were less pronounced in anti-*PROPEP3* immunoblots, our results indicate that Pep-induced *PROPEP3* release is increased in the absence of BAK1. Under our conditions, we failed to detect endogenous *PROPEP3* or a small, possibly processed form of *PROPEP3*-Venus. These data suggest that *PROPEP3* can be released without extensive processing.

We next tested whether *BAK1* disruption influences PEPR accumulation. PEPR1-FLAG transgenic plants recapitulated the observed *bak1* effects on *PR1* and *PDF1.2a* induction in response to Pep2, without significantly affecting steady-state receptor accumulation (Fig EV4A and B). In the presence of BAK1, Pep1 but not flg22 application leads to a transient decline of PEPR1-FLAG accumulation

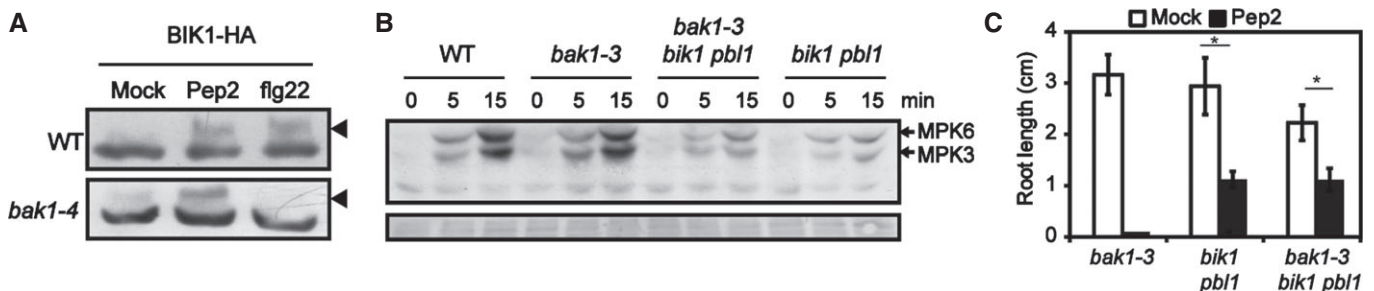


Figure 2. BIK1-dependent sensitization of PEPR signaling in the absence of BAK1.

A Immunoblot analysis for BIK1-HA in *Arabidopsis* protoplasts exposed to Pep2 or flg22 for 10 min. Arrowheads indicate phosphorylated BIK1-HA.
 B Immunoblot analysis for Pep2-triggered MAPK activation. Ponceau S-stained loading controls are shown (bottom).
 C Root length (averages \pm SD, $n \geq 15$) of *Arabidopsis* seedlings that were exposed to 100 nM Pep2. * $P < 0.05$ in two-tailed tests compared to the differences (\pm Pep2) from the corresponding values of *bak1-3* plants. Two independent experiments were combined for statistical analysis.

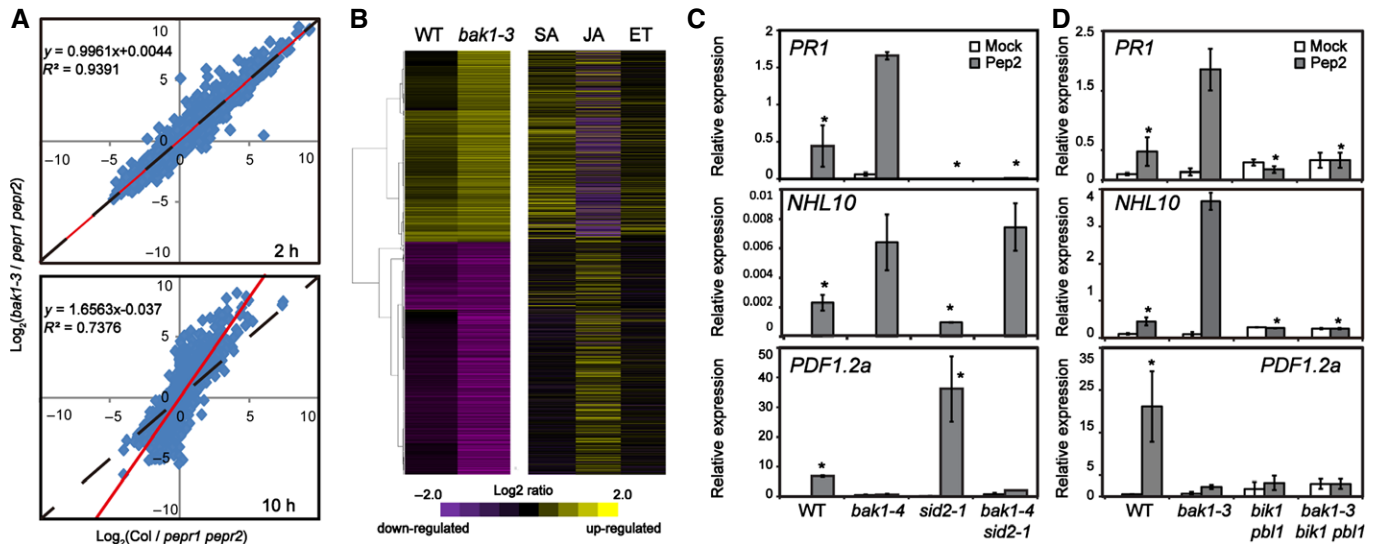


Figure 3. BAK1 disruption leads to reprogramming of PEPR-mediated defense outputs.

- A Scatter plots for \log_2 fold changes of gene expression in WT plants versus *bak1-3* plants treated with Pep2 for 2 and 10 h. The regression of these scatter plots is indicated by the red lines.
- B Hierarchical analysis of genes exhibiting a > two-fold change in expression level in *bak1-3* plants after Pep2 application for 10 h in a whole-genome microarray analysis. Using Genevestigator v3, these genes were separately cross-referenced to public databases to show their expression responses to salicylate (SA), methyl jasmonate (JA), or ethylene (ET).
- C, D qRT-PCR analysis of defense-related genes in 10-day-old seedlings exposed to 0.5 μ M Pep2 for 10 h. Data are averages (\pm SD) of three biological replicates. * P < 0.05 in two-tailed tests compared to the corresponding *bak1-4* and *bak1-3* values in (C) and (D), respectively. Relative cycle threshold (C_t) values of two independent experiments were combined for statistical analysis.

by ~50% within 5 h (Fig 4C), without significantly lowering the transcript levels (Fig EV4C). In the absence of BAK1, however, the receptor accumulation remained unaltered over the tested time course after Pep1 application (Fig 4D). Ligand-induced PEPR1-FLAG down-regulation was also blocked in the presence of the proteasome inhibitor MG132 (Rock *et al.*, 1994), or the endocytosis inhibitors Wortmannin (Emans *et al.*, 2002) and Tyrphostin A23 (Banbury *et al.*, 2003) (Fig 4E). These results suggest that Pep1 induces the proteasomal degradation of PEPR1, in association with BAK1-dependent internalization, as previously described for FLS2 (Chinchilla *et al.*, 2007; Smith *et al.*, 2014). Stabilization of a ligand-elicited receptor pool may prolong Pep responses in *bak1*-KO plants.

BAK1 and BON proteins control the balance of SA- and JA-related outputs in PEPR signaling

We further addressed the mechanisms by which BAK1 disruption influences the balance between different PEPR-mediated defense outputs. Of the tested *bak1 serk* double mutants, Pep2 induction of *PR1* and *NHL10* was further enhanced in *bak1 bkk1* plants (Fig EV2F), pointing to a correlation between cell death de-repression (He *et al.*, 2007) and defense reprogramming.

This prompted us to assess whether loss of BON proteins recapitulates the *bak1*-like cell death phenotype. In *bon1 bon2* and *bon1 bon3* plants, Pep2 induction of *PR1* and *NHL10* was much further enhanced, while that of *PDF1.2* was lowered, compared to WT plants (Fig 5A). Pep2-induced *PR1* induction was much higher in *bon* mutant plants than in *bak1-4* plants (see the difference in scales between Figs 3C and 5A), which may be attributable to the

previously described constitutive sensitization of SA-related defenses in *bon* plants (Yang *et al.*, 2006; Fig 5A). Pep2-induced growth inhibition was also stronger in *bon1 bon2*, and *bon1 bon3* plants than in WT plants (Fig 5B). In good accordance, the dwarfism of *bon1* plants was again alleviated in the absence of PEPRs (Fig 5C), pointing to a contribution of endogenous PROPEP-PEPR signaling to cell death in plants lacking BON1. Our results thus indicate that the removal of the BAK1/BON pathway redirects PEPR signaling to the potentiation of SA-related defenses and cell death. We further showed that BAK1 accumulation was retained in *bon1 bon2* and *bon1 bon3* plants (Fig 5D), excluding the possibility that the *bon* phenotype is caused by reduced BAK1 accumulation.

Virulence effector-dependent production of PROPEP proligands

To assess the biological relevance of our findings, we traced the production and possible extracellular release of PROPEP proligands after pathogen challenge. Of PROPEP1-PROPEP6, PROPEP3 and PROPEP2 were massively induced upon challenge with the bacterial phytopathogen *Pseudomonas syringae* pv. *tomato* (Pst) DC3000 (Figs 6A and EV5A). There were two phases of PROPEP2/PROPEP3 induction over the time course tested, although the first (2 h post-inoculation (hpi)) was less pronounced for PROPEP2 (Fig 6A). The second phase (24 hpi) was almost abolished (or, possibly, much delayed) following challenge with Pst DC3000 Δ hrcC, which is deficient in type III effector (T3E) secretion (Yuan & He, 1996), as well as following flg22 application (Figs 6A and EV5B). Our results thus suggest that the bacterial MAMPs and virulence effectors,

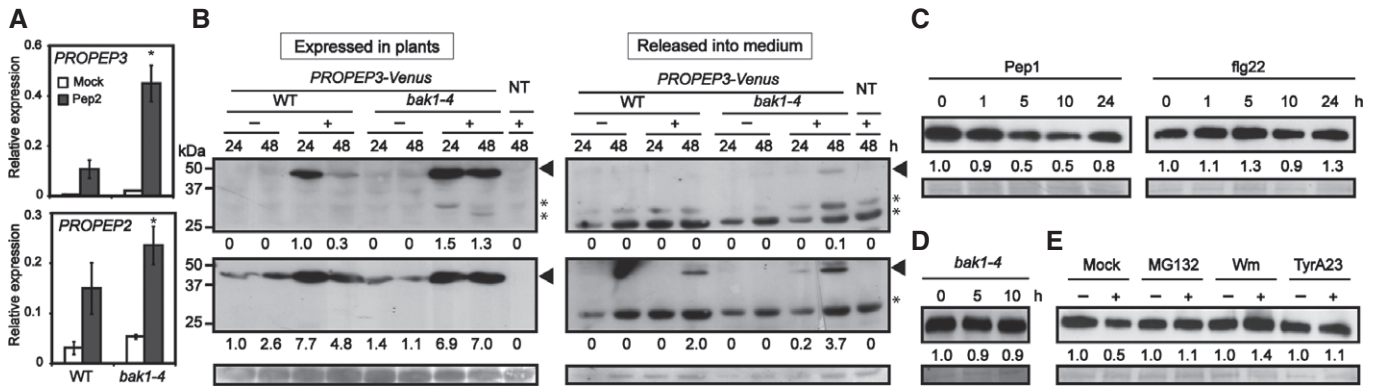


Figure 4. PROPEP proligand production and PEPR1 accumulation following Pep application are reinforced in the absence of BAK1.

A qRT-PCR analysis of *PROPEP* genes in 10-day-old seedlings exposed to 0.5 μ M Pep2 for 10 h. * $P < 0.05$ in two-tailed tests compared to the corresponding WT values. Relative C_t values of two independent experiments with three biological replicates each were combined for statistical analysis. Data are averages (\pm SD) of three biological replicates.

B Anti-GFP (upper) and anti-PROPEP3 (middle) immunoblot analysis of PROPEP3-Venus in seedlings submerged in liquid medium and treated with (+) or without (–) 0.5 μ M Pep2 for the indicated times. The positions of the molecular weight markers are shown on the left. Arrowheads and asterisks indicate PROPEP3-Venus and cross-reactive bands, respectively.

C–E Immunoblot analysis of PEPR1-FLAG in 10-day-old seedlings following Pep1 or flg22 application. (C, D) Plants were exposed to 1 μ M Pep1 or flg22 for the indicated times. (E) Plants were pre-exposed to MG132 (50 μ M), Wortmannin (Wm) (30 μ M), and Tyrphostin A23 (TyrA23) (100 μ M) for 1 h before being exposed to Pep1 for 10 h.

Data information: The numbers below the immunoblots represent relative intensities of the PROPEP-Venus (B) and PEPR1-FLAG (C–E) bands normalized to the backgrounds in the Ponceau S-stained loading controls (bottom), with the band/background values in WT plant extracts 24 h (upper) and 0 h (middle) after Pep2 application, respectively, set as 1.0.

respectively, greatly contribute to the first and second phases of the proligand induction at the mRNA level.

PROPEP2/PROPEP3 induction in response to flg22 and *Pst* DC3000 Δ hrcC was lowered in *bak1*-KO plants (Fig EV5B and C). A BAK1-dependent receptor(s) may predominantly contribute to PROPEP3 production in response to bacterial MAMPs, as previously shown for stomatal closure during bacterial challenge (Zeng & He, 2010). However, WT-like *PROPEP2/PROPEP3* induction was restored in *bak1* plants after *Pst* DC3000 inoculation (Fig EV5D). These data suggest that BAK1 is required for MAMP-dependent induction of the proligands, but becomes dispensable for effector-dependent induction during bacterial challenge. PEPRs *per se* were dispensable for *PROPEP2/PROPEP3* induction in response to *Pst* DC3000 in both WT and *bak1-4* backgrounds (Fig EV5D), pointing to robustness of the proligand production.

Our immunoblot analysis revealed that PROPEP3-Venus protein accumulation largely reflected *PROPEP3* induction as described above. In *bak1-4* plants, early PROPEP3-Venus accumulation was reduced in response to *Pst* DC3000 Δ hrcC, but it was unaffected in response to *Pst* DC3000 (Fig 6B). These results confirm the BAK1 independence of PROPEP3 production in plants exposed to bacterial T3Es.

PROPEP3-Venus accumulation was sustained for at least 48 h in response to *Pst* DC3000 and was largely indistinguishable between WT and *bak1-4* plants (Fig 6C). Unlike in Pep-treated plants (Fig 4B), we detected two small forms of PROPEP3-Venus, in addition to the most abundant, apparently full-length form, at 24 and 48 h after inoculation (Fig 6C left). Whether they were produced inside or outside the cell remains to be determined. Of particular note, in the extracellular fraction, the smallest form (~30 kDa) of PROPEP3-Venus predominantly accumulated during bacterial challenge (Fig 6C right). Extracellular release of PROPEP3-Venus was again increased in *bak1-4* plants, despite no significant increase in

the proligand production *in planta* (Fig 6C). We observed enhanced cell death in *bak1-4* plants, compared to WT plants, following *Pst* DC3000 challenge (Fig 6D), as described previously (He *et al*, 2007; Kemmerling *et al*, 2007). These results suggest that, in the absence of BAK1, enhanced cell death leads to an increase in the extracellular release of the proligand (Fig 6C).

Together with this, the previously described role for PEPR in coupling ETI with systemic immunity (Ross *et al*, 2014) prompted us to test whether cell death associated with ETI also stimulates PROPEP3 release. We observed massive cell death and high PROPEP3-Venus accumulation 48 h after inoculation with an avirulent strain of *Pst* DC3000, *AvrRpm1* (Fig 6D and E left). As well as during basal resistance to *Pst* DC3000 (Fig 6E right), we again detected the two small forms, in addition to the apparently full-length form, of PROPEP3-Venus. PROPEP3-Venus was also released during ETI, predominantly in the smallest form. Given the retention of the Venus epitope in the released small form (Fig 6F), PROPEP3-Venus likely underwent N-terminal truncation following bacterial challenge as deduced previously (Huffaker *et al*, 2006).

PEPRs are required for basal resistance in *bak1*-knockout plants

We next assessed a role for the PEPR pathway in pathogen resistance in the presence or absence of BAK1. *pepr1 pepr2 BAK1* (+) plants were essentially indistinguishable from WT plants in their basal resistance to the virulent Noco2 strain of the oomycete phytopathogen *Hyaloperonospora arabidopsidis* (*Hpa*) (Fig 7A), as shown for post-invasion resistance to *Pst* DC3000 (Ross *et al*, 2014). The growth of *Hpa* Noco2 was reduced in *bak1* plants as described previously (Kemmerling *et al*, 2007), but was substantially permitted in *bak1 pepr1 pepr2* plants (Fig 7A). We also assessed post-invasion resistance to *Pst* DC3000 in these plants following leaf infiltration of

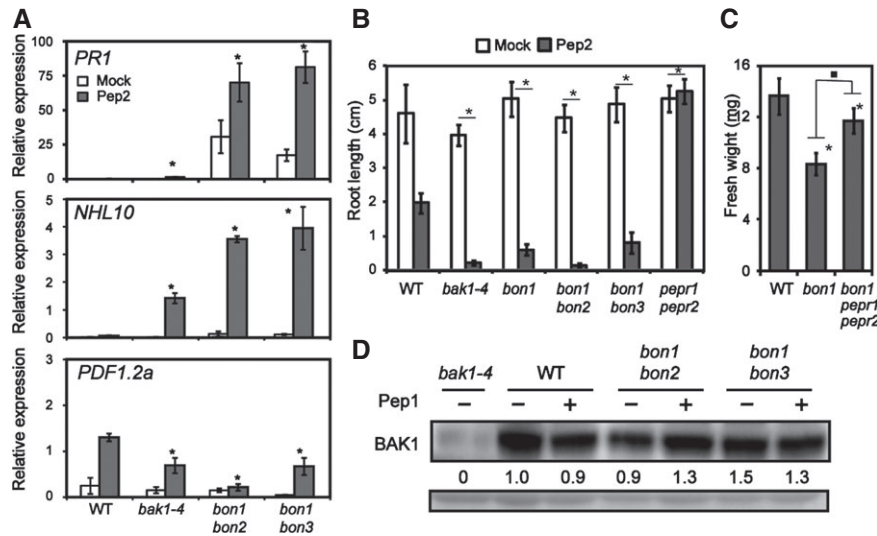


Figure 5. Reprogramming of PEPR-mediated defense outputs upon disruption of BAK1/BON-mediated cell death suppression.

- A** qRT-PCR analysis of defense-related genes in 10-day-old seedlings exposed to 0.5 μ M Pep2 for 10 h. $*P < 0.05$ in two-tailed tests compared to the corresponding WT values. Relative C_t values of two independent experiments with three biological replicates each were combined for statistical analysis. Data are averages (\pm SD) of three biological replicates.
- B** Root length (averages \pm SD, $n \geq 15$) of *Arabidopsis* seedlings exposed to 100 nM Pep2. $*P < 0.05$ in two-tailed tests compared to the differences (\pm Pep2) from the corresponding values of WT plants. Two independent experiments were combined for statistical analysis.
- C** Fresh weight (averages \pm SD, $n \geq 25$) of 2-week-old plants grown on soil. $*P < 0.05$ in two-tailed tests compared to the corresponding values of WT plants. $\blacksquare P < 0.05$ in two-tailed tests. Two independent experiments were combined for statistical analysis.
- D** Immunoblot analysis for BAK1 in 10-day-old seedlings with or without 0.5 μ M Pep1 for 24 h. The numbers below the upper panel represent relative intensities of the BAK1 band normalized to the backgrounds in the Ponceau S-stained loading controls, with the value in non-elicited WT plants set as 1.0.

the bacteria, under conditions in which a contribution of leaf surface immunity can be essentially ignored. The growth of the bacteria was limited in (mock-treated) *bak1* plants, but was again increased in *bak1 pepr1 pepr2* plants (Fig 7B). These results indicate a critical role for PEPRs in basal resistance in the absence of BAK1.

flg22-induced resistance, which is entirely dependent on FLS2 (Zipfel et al, 2004), was largely unaffected in *bak1-4* and *pepr1 pepr2* plants under our conditions (Fig 7B). Notably, however, flg22-induced resistance almost collapsed in *bak1-4 pepr1 pepr2* plants (Fig 7B). Correlated with this, flg22-induced SA production and *PR1* activation remained unaffected in *bak1-4* and *pepr1 pepr2* plants, but both were lowered in *bak1-4 pepr1 pepr2* plants (Fig 7C and D), without a significant decrease in steady-state FLS2 accumulation (Fig EV5E). It should be noted that even *bak1-KO* plants displayed reduced but detectable *PROPEP2/PROPEP3* induction in response to flg22 (Fig EV5B). We infer from these results that, once weakened FLS2 signaling is linked to PEPR signaling, which then sustains SA-based defenses in the absence of BAK1. Consistent with this model, we found that *SID2* was required for bacterial resistance in *bak1-4* plants, with or without flg22 treatment (Fig 7E). Moreover, loss of BAK1 increased bacterial resistance even in the *sid2* background (Fig 7E), pointing to an enhancement of SA-independent defense in *bak1-KO* plants. Whether this also requires PEPRs remains to be determined.

We further showed that elf18-triggered *PR1* and *FRK1* induction was elevated in *bak1-4* plants compared to WT plants, yet the *bak1* effects were abolished in the absence of PEPRs (Fig EV5F). This was also the case for *PR1* induction upon *Pst* DC3000 Δ hrpC inoculation in *bak1-4* plants (Fig EV5G). These results suggest that, upon BAK1

disruption, the PEPR pathway not only reinstates suppressed MAMP receptor pathways but also boosts those that are less affected.

BAK1 depletion during *Colletotrichum higginsianum* challenge renders PEPRs essential in anti-fungal resistance

Our findings above would be of relevance if BAK1 depletion occurred during pathogen challenge. BAK1 accumulation was retained following challenge with *Pst* DC3000 and *Pst* DC3000 *AvrRpm1* (Fig EV5H), consistent with WT-like basal resistance and ETI of *pepr1 pepr2* BAK1 (+) plants (Fig 7B mock; Ross et al, 2014), respectively. However, we found that *Ch* resistance was significantly lowered in *pepr1 pepr2* BAK1 (+) plants at 5 days post-inoculation (dpi) (Fig 8A left). This could be accounted for if the cellular supply of BAK1 was lowered during *Ch* resistance. Indeed, the accumulation of BAK1, but not of PEPR1-FLAG or MPK3, was substantially reduced 4 days after *Ch* challenge (Fig 8B). This seems to occur at the post-transcriptional level, given the unaltered *BAK1* mRNA accumulation (Fig 8B). The specific decrease in BAK1 protein accumulation precludes the possibility that it merely reflects a consequence of necrotrophic cell death caused by *Ch* infection. Therefore, our results indicate that BAK1 depletion indeed occurs during *Ch* infection and thereby renders the PEPR pathway necessary for basal resistance.

We further revealed that *bak1-4* plants enhanced both the rate of successful *Ch* invasion and fungal growth (assessed by lesion size) (Fig 8A), pointing to the existence of a BAK1-dependent step in anti-fungal resistance. By contrast, loss of PEPRs did not increase fungal invasion rate, which was determined at 3 dpi (Fig 8A right), before

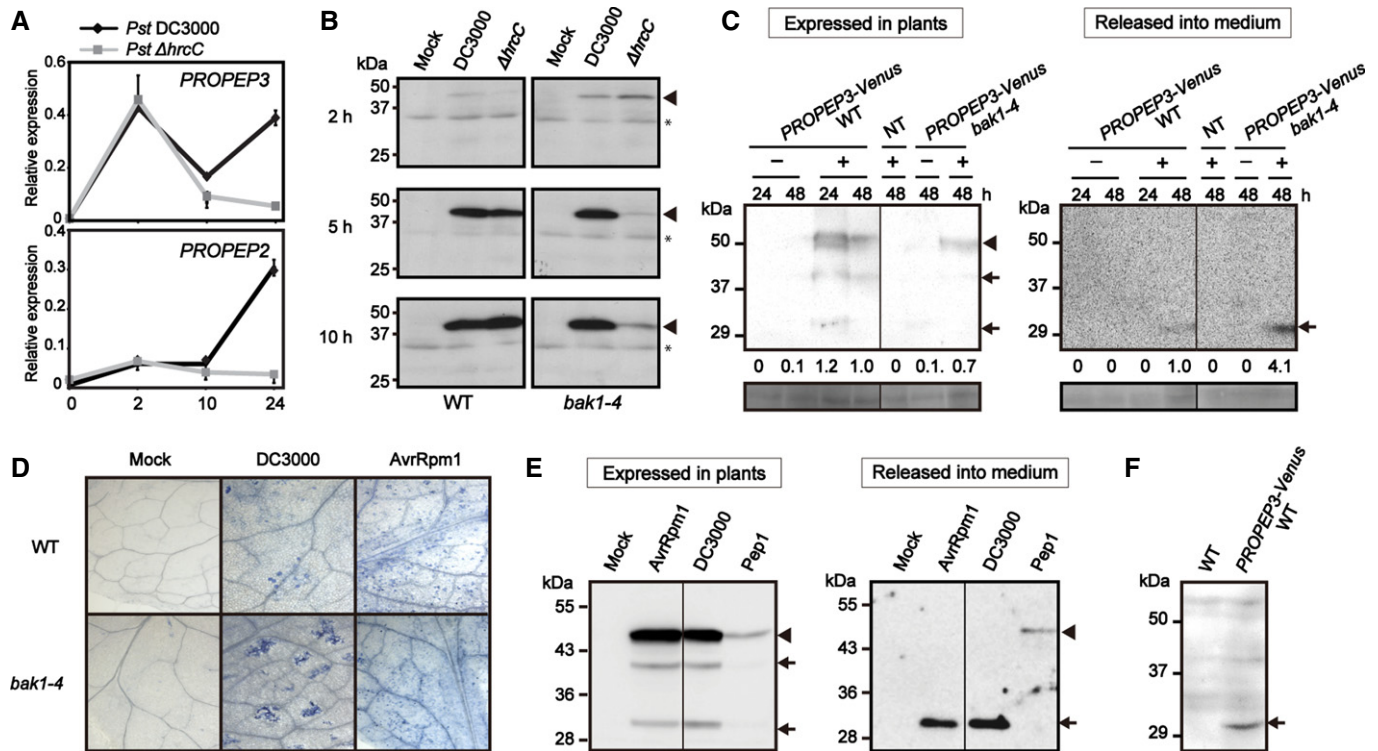


Figure 6. PROPEP production and release during bacterial resistance.

A qRT-PCR analysis in 4-week-old plant leaves challenged with the indicated *P. syringae* pv. *tomato* (*Pst*) DC3000 strains for the indicated times. Data are averages (\pm SD) of three biological replicates.

B Anti-GFP immunoblot analyses in seedlings challenged with *Pst* DC3000 (DC3000) and *Pst* DC3000 Δ hrcC (Δ hrcC) for the indicated times.

C Anti-PROPEP3 immunoblot analysis of PROPEP3-Venus (upper) in plant tissues (expressed in plants) and in the extracellular fraction (released into medium), 24 and 48 h after the inoculation with (+) or without (–) *Pst* DC3000. Lower panels indicate Ponceau S-stained loading controls. The numbers below the upper panel represent relative intensities of the PROPEP3-Venus band normalized to the backgrounds in the Ponceau S-stained loading controls. NT denotes non-transgenic WT plants.

D Trypan blue cell death staining of *Arabidopsis* seedlings challenged with *Pst* DC3000 or *Pst* DC3000 *AvrRpm1* (*AvrRpm1*) for 48 h.

E Anti-PROPEP3 immunoblot analyses in the seedlings exposed to the indicated *Pst* DC3000 strains or 1 μ M Pep1 for 48 h.

F Anti-GFP immunoblot analysis for the extracellular fraction of the seedlings exposed to *Pst* DC3000 *AvrRpm1* for 48 h.

Data information: In (B, C, E, and F), arrowheads and arrows indicate an apparently full-length and processed form of PROPEP3-Venus, respectively. Asterisks indicate cross-reactive bands. The positions of the molecular weight markers are shown on the left of the immunoblots.

Source data are available online for this figure.

BAK1 was substantially depleted (Fig 8B). These results suggest that *Ch*-induced BAK1 depletion contributes to the suppression of invasion resistance but results in PEPR-dependent post-invasion resistance. Importantly, we again observed that loss of PEPRs further reduced overall fungal resistance in the absence of BAK1 (Fig 8A left). This strengthens our contention that the PEPR pathway plays a critical role in basal resistance in plants depleted of BAK1.

Discussion

As a shared co-receptor for different PRRs, BAK1 may represent an Achilles heel in plant immunity. A key question involves how plants display effective resistance in response to or in the presence of pathogen assaults on BAK1. This is of crucial relevance in light of the range of pathogen effectors that target the co-receptor. The present study reveals that the PEPR pathway is engaged and rewired in response to MAMPs, pathogen effectors, and BAK1 depletion and thereby leads to basal resistance (Fig 9).

In *Arabidopsis*-*Pst* compatible interactions, we discovered that these three elements collectively contribute to the production of the PROPEP proligands, a prerequisite for PEPR signaling activation. As shown with *PROPEP2*/*PROPEP3* and *PROPEP3*-Venus, an initial MAMP-triggered induction is followed by further induction dependent on bacterial T3Es. On the other hand, sustained *PROPEP2*/*PROPEP3* induction was previously detected in seedlings treated with elf18 (Tintor *et al.*, 2013). The apparent discrepancy may be attributable to differences in the MAMPs and/or plant tissues used. Nevertheless, the present data show that *Pst* virulence effectors increase the production of the proligands as compared to their production in response to MAMPs alone. This seems not merely to reflect vigorous bacterial growth, given the potent *PROPEP3*-Venus production despite the termination of bacterial growth in ETI (Belkadir *et al.*, 2004). It is also notable that effector-dependent *PROPEP2*/*PROPEP3* induction overcomes the requirement for BAK1 in MAMP-dependent induction. This likely underlies the engagement of the PEPR pathway in basal resistance in the absence of BAK1. Moreover,

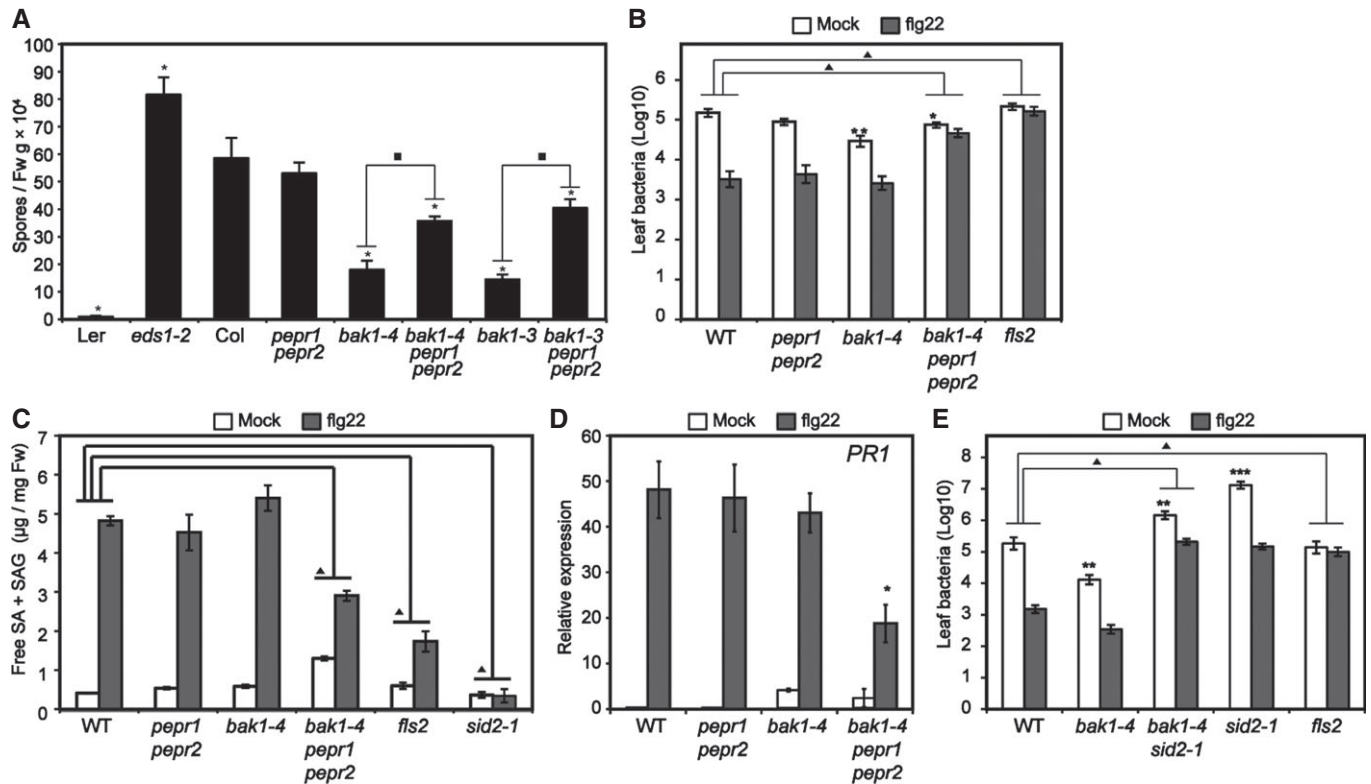


Figure 7. PEPRs are required to mount SA-dependent basal resistance in the absence of BAK1.

- A** Growth of *H. arabidopsidis* (*Hpa*) Noco2 in 2-week-old plants. Spores were counted at 6 days post-inoculation (dpi). Results are averages \pm SE of three biological replicates. * $P < 0.05$ in two-tailed tests compared to the corresponding values of Col plants. ■ $P < 0.05$ in two-tailed tests between the indicated values. Three independent experiments were combined for statistical analysis.
- B** Growth of syringe-infiltrated *Pst* DC3000 in rosette leaves of 4-week-old plants pretreated with water (Mock) or 1 μ M flg22 for 24 h. Bacterial titers were determined at 3 dpi. Results are averages \pm SE of three independent replicates. * $P < 0.05$ and ** $P < 0.01$ in two-tailed tests compared to the corresponding values of WT plants. ▲ $P < 0.01$ in two-tailed tests compared to the differences (\pm flg22) from the corresponding values of WT plants. Three independent experiments were combined for statistical analysis.
- C** Total SA levels were determined in the rosette leaves of 4-week-old plants with or without 1 μ M flg22 application for 24 h. Data are averages (\pm SD) of material from three independent plants. The experiments were repeated twice, with similar results. ▲ $P < 0.01$ in two-tailed tests compared to the differences (\pm flg22) from the corresponding values of WT plants. Two independent experiments were combined for statistical analysis.
- D** qRT-PCR analysis of the *PR1* gene in 4-week-old plants exposed to 1 μ M flg22. Data are averages (\pm SD) of three biological replicates. * $P < 0.05$ in two-tailed tests compared to the corresponding WT values. Relative C_t values of four independent experiments were combined for statistical analysis.
- E** Growth of syringe-infiltrated *Pst* DC3000 in rosette leaves of 4-week-old plants pretreated with water (Mock) or 1 μ M flg22 for 24 h. Bacterial titers were determined at 3 dpi. Results are averages \pm SE of three independent replicates. ** $P < 0.01$ and *** $P < 1.0 \times 10^{-10}$ in two-tailed tests compared to the corresponding values of WT plants. ▲ $P < 0.01$ in two-tailed tests compared to the differences (\pm flg22) from the corresponding values of WT plants. Three independent experiments were combined for statistical analysis.

PEPR-independent PROPEP production on exposure to bacterial effectors further increases robustness of the proligand production. This may enable non-cell-autonomous PEPR signaling from cells displaying damaged and impaired receptor function to the surrounding cells.

Remarkably, PROPEP3 release during *Pst* basal resistance is increased upon BAK1 disruption, apparently in association with elevated cell death, demonstrating that at least PROPEP3 (or its derivatives) provides a DAMP, indicative of membrane disintegration associated with pathogen challenge. This presents, for the first time, compelling evidence that the PEPR pathway acts in DAMP sensing and signaling during plant immunity. Given the previously described PEPR requirement for MAMP responses in sterile seedlings (Ma et al, 2012; Tintor et al, 2013), PROPEP release should occur to some extent upon exposure to MAMPs alone. The present

study illustrates that, following MAMP-dependent induction, pathogen effectors and BAK1 depletion additively enhance the generation and release of the proligands. Furthermore, predominant accumulation of a putatively processed small form of PROPEP3-Venus in the extracellular space following exposure to bacterial effectors (or bacterial pathogens) implies the existence of an additional regulatory step in the activation of PEPR ligands. Of particular note, this form was apparently absent in plants treated with Pep1 or Pep2, pointing to an association between its formation and pathogen challenge. Future studies will be required to determine the identity and biological significance of this apparently processed form(s) of PROPEP3, and also the possible involvement of a protease produced by the modified host or the invading bacteria. Nevertheless, such stepwise reinforcement of extracellular PROPEP supply is reminiscent of the danger hypothesis, in which sensing host damage

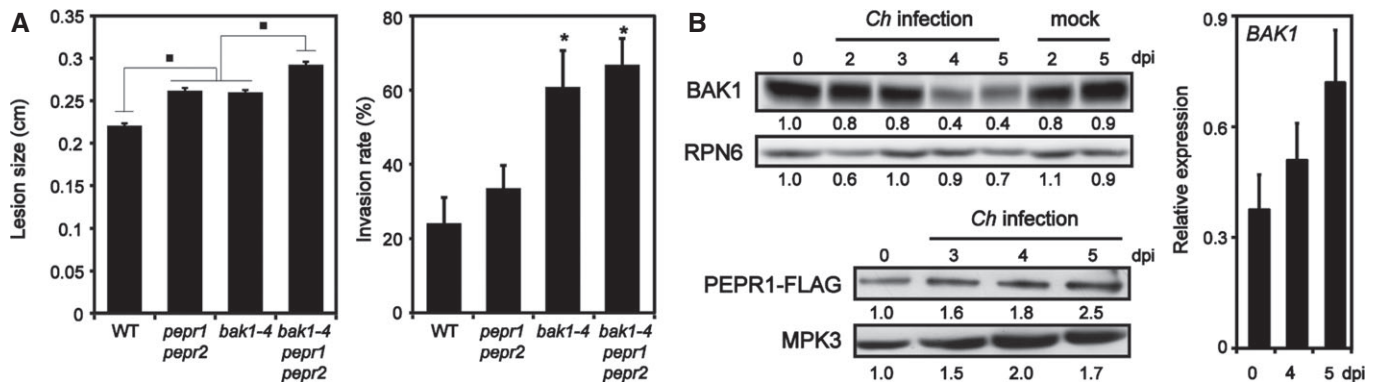


Figure 8. BAK1 is depleted during *C. higginsianum* infection.

A Lesion sizes (left) were determined 5 days after *C. higginsianum* (*Ch*) spore inoculation. Invasion rates (right) of *Ch* on *Arabidopsis* leaves were determined 3 days after spore inoculation. An average of three replicates is shown (\pm SD) (left) and (\pm SE) (right). \blacksquare $P < 0.05$ in two-tailed tests between the indicated samples. $\ast P < 0.05$ in two-tailed tests compared to the corresponding WT values. Two independent experiments were combined for statistical analysis.

B Immunoblot (left) and qRT-PCR (right) analyses following *Ch* challenge for the indicated times (dpi). The numbers below the immunoblots represent relative intensities of the indicated bands normalized to the backgrounds, with the values at 0 dpi set as 1.0. Experiments were performed three times with the same conclusions.

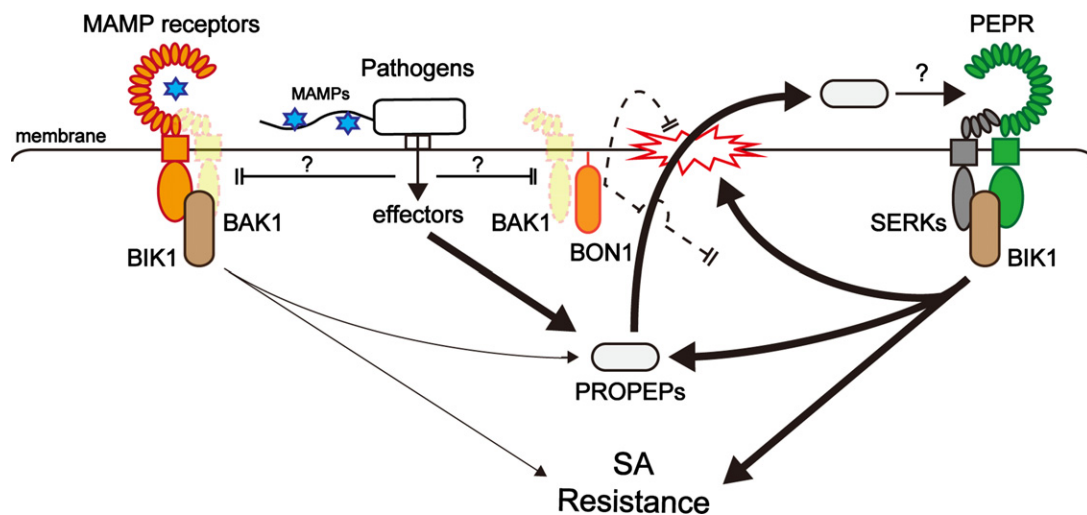


Figure 9. A model for PEPR-mediated basal resistance following the removal of BAK1-/BON-mediated control.

Following BAK1 depletion, possibly by pathogen effector actions, MAMP-triggered outputs including induction of PROPEPs are weakened. However, effector-dependent PROPEP induction compensates for low amounts of MAMP-induced PROPEPs in the absence of BAK1. Cell death spread following dysfunction of BAK1-/BON-mediated control probably facilitates release of cytosolic PROPEPs into the extracellular space. Moreover, in the absence of BAK1/BON1 complexes, PEPR signaling is strengthened by the stabilization of the receptor and by the potentiation of SA-related defenses toward anti-biotrophic resistance.

(DAMPs) associated with pathogen infection, in addition to MAMPs, is critical for robust defense activation (Stuart *et al*, 2013). It should be also noted that release of the small PROPEP3 form into the extracellular space also occurs without BAK1 depletion during and/or after ETI. Our results thus clearly show that BAK1 depletion is not essential for PROPEP3 release, but positively influences this important step during basal resistance. ETI activation, possibly in association with cell death, may offer an alternative to BAK1 depletion for the stimulation of the DAMP pathway.

At present, it remains unclear whether PROPEP processing facilitates PEPR recognition. Nonetheless, we show that Pep-induced PROPEP3 generation and subsequent release is also strengthened

upon BAK1 disruption, in a manner dependent on PEPRs. This predicts that if active ligands are supplied in the absence of BAK1, PEPR signaling leads to cell death and is maintained by positive auto-feedback, thereby sustaining basal resistance.

We further revealed that BAK1 depletion and catalytic inactivation, respectively, lead to sensitization and desensitization of PEPR-mediated cell death and defense responses. Given the differential requirements for BAK1 kinase activity between cell death and PRR signaling (Schwessinger *et al*, 2011), BAK1 kinase suppression is likely to block PEPR signaling without de-repressing pro-death signaling. In agreement with this, different bacterial effectors have been reported to target BAK1 and/or PRR partners through

physical associations (Macho & Zipfel, 2015). AvrPto inhibits FLS2/EFR kinase activity and may also block PRR-BAK1 associations (Shan *et al*, 2008; Xiang *et al*, 2008, 2011). AvrPtoB is able to suppress FLS2-BAK1 association and kinase activity of BAK1 (Shan *et al*, 2008; Cheng *et al*, 2011). HopAO1 phosphatase reverses critical phosphorylation on a tyrosine residue of EFR that is conserved in many RKs including FLS2, BAK1, and PEPR1/PEPR2 (Macho *et al*, 2014). On the other hand, HopU1 mono-ADP ribosyltransferase reduces FLS2/EFR accumulation by inhibiting specific binding of the RNA-binding protein GRP7 to *FLS2/EFR* but not *BAK1* transcripts (Nicaise *et al*, 2013). Although it is possible that AvrPtoB-mediated BAK1 ubiquitination (Goehre *et al*, 2008) leads to BAK1 degradation, the unaltered BAK1 accumulation and the low PROPEP3-Venus release that we observed in *BAK1* (+) plants during *Pst* challenge imply that *Pst* predominantly inhibits BAK1/PRR activity without significantly affecting BAK1 abundance. This strategy may have been selected to minimize de-repression of PEPR and parallel DAMP signaling, given that *Pst* indeed eliminates other host targets by T3Es, for example, PBS1 by AvrPphB and RIN4 by AvrRpt2 (Shao *et al*, 2003; Kim *et al*, 2005a).

In contrast, *Ch* infection is accompanied by a substantial decrease in BAK1 accumulation, which likely serves to overcome BAK1-dependent defenses. However, this also seems to result in the stimulation of PEPR-mediated post-invasion defenses. This model well illustrates the observed separation between PEPR-dependent and -independent steps during basal *Ch* resistance. Future studies will address whether and how a fungal effector(s) mediate specific BAK1 depletion.

This study reveals that BAK1 depletion and consequent dysfunction of BAK1/BON-mediated control leads to active engagement and rewiring of the PEPR pathway toward cell death and anti-biotrophic resistance (Fig 9). Previous genetic studies showed that pro-death pathways, distinct from the PEPR pathway in SA and EDS1/PAD4 dependence, are derepressed when BIR1, BIR2, or BON functions are compromised (Yang *et al*, 2006; Gao *et al*, 2009; Halter *et al*, 2014). At least one such pathway requires the LRR-RK SOBIR1 (Gao *et al*, 2009), which functions with different LRR receptor-like proteins to mount anti-fungal resistance (Gust & Felix, 2014; Liebrand *et al*, 2014). However, it was previously shown that PEPR function is retained in the absence of an N-glycosylation-dependent ER quality control (QC) pathway, while in contrast, SOBIR1 function is impaired (Saijo, 2010; Tintor *et al*, 2013; Sun *et al*, 2014; Zhang *et al*, 2015), indicating that SOBIR1 function is not required for PEPR function. These findings point to the notion that a wide array of defense pathways, differing in ER QC requirements, is under BAK1/BON-mediated attenuation. This is in good agreement with the hypothesis that the disintegration of BAK1/BON complexes is sensed and linked to robust defense activation (Gao *et al*, 2009; Halter *et al*, 2014). Whether and how these separate defense pathways become engaged in resistance following pathogen-induced BAK1 depletion requires further investigation.

Mounting evidence indicates that defects in different MTI components, including BAK1, BIK1, the NADPH oxidase RbohD, MPK4, and the callose synthase PMR4, enhance basal resistance against virulent (hemi-)biotrophic pathogens (Nishimura *et al*, 2003; Kim *et al*, 2005b; Zhang *et al*, 2010, 2012; Laluk *et al*, 2011; Kadota *et al*, 2014; Roux *et al*, 2015). Studies on natural variation in

Arabidopsis-Hpa interactions point to the prevalence of intermediate resistance based on interactions between multiple host-pathogen components (Krasileva *et al*, 2011). Although BAK1 depletion results in PEPR-mediated basal resistance, strict BIK1 requirement excludes the DAMP pathway from the resistance activated in *bik1* plants (Zhang *et al*, 2010; Laluk *et al*, 2011). Multilayered engagement of different DAMP pathways, possibly in response to effector-mediated interference in MAMP signaling, is likely to underlie basal resistance against virulent pathogens.

Materials and Methods

Plant materials and growth conditions

WT plants used were *Arabidopsis thaliana* Col-0 unless otherwise stated. *pepr1-1* (SALK_059281) and *pepr2-3* (SALK_098161); *bak1-3* and *bak1-4* (Chinchilla *et al*, 2007); *bak1-7*, *bak1-8*, and *bak1-10* (in the Aeq cyt background); *bak1-13*, *bak1-14*, and *bak1-15* (in the Aeq vmd background) (Ranf *et al*, 2012); *bak1-5*, BAK1pro:BAK1/*bak1-4* and BAK1pro:BAK1(D416N)/*bak1-4* (Schwessinger *et al*, 2011); *sid2-1* (Wildermuth *et al*, 2001); *eds1-2* and *lsd1c* (Rustérucci *et al*, 2001); *fls2* (Zipfel *et al*, 2004); *bon1-1*, *bon2-2*, and *bon3-3* (Yang *et al*, 2006); *serk1-1*, *serk1-3*, *serk2-2*, *bkk1-1*, *serk5-1*, and 35Spro: BES1D/*serk1-3 bak1-3* (Albrecht *et al*, 2008); *bri1-301* (Nam & Li, 2002); and *PROPEP3pro*:PROPEP3-Venus (Ross *et al*, 2014) were used. *PROPEP3pro*:PROPEP3-Venus/*bak1-4* was generated by crossing. Plants were grown on soil or 0.5 × Murashige and Skoog (MS) medium containing 25 mM sucrose, under 10 h light/14 h dark or 12 h light/12 h dark, respectively, unless otherwise stated.

Plant transformation

The genomic DNA sequences of the *PEPR1* (At1 g73080) loci including the intergenic and coding regions were inserted into the binary vector pAM-PAT for expressing their C-terminal FLAG fusions and then introduced into *pepr1 pepr2* plants via *Agrobacterium*-mediated transformation.

Microbial materials

The *ΔhrcC* (Yuan & He, 1996) and *AvrRpm1* (Debener *et al*, 1991) strains of *Pseudomonas syringae* pv. *tomato* (*Pst*) DC3000 (Dong *et al*, 1991), Noco2 strain (Parker *et al*, 1993) of *Hyaloperonospora arabidopsidis* (*Hpa*), and IMI 349063A strain (O'Connell *et al*, 2004) of *Colletotrichum higginsianum* (*Ch*) were used in this study.

Bioassay for pattern-triggered responses

For root growth assays, 2-day-old seedlings were treated with 100 nM Pep2 in liquid medium for 7 days, before measuring root length or staining with Evans blue or lactophenol trypan blue. For MAPK assays, 10-day-old seedlings were treated for the indicated times with 1 μM Pep2 or flg22. Proteins were extracted in an extraction buffer (50 mM Tris-HCl pH 7.5, 200 mM NaCl, 1 mM EDTA, 10 mM NaF, 25 mM beta-glycerophosphate, 2 mM sodium orthovanadate, 10% glycerol, 2 mM DTT, 1 mM PMSF, 1% (v/v) P9599 protease inhibitor cocktail (Sigma)). The

supernatants were recovered after centrifugation at 17,000 *g* for 15 min at 4°C and then subjected to immunoblot analysis on 10% SDS–PAGE with rabbit anti-p44/42 MAPK antibodies (Cell Signaling). For qRT–PCR analysis, 10-day-old seedlings were exposed to the indicated elicitors for the indicated times, unless otherwise stated. The PCR primers used were described previously (Tintor *et al*, 2013; Ross *et al*, 2014).

Pathogen inoculation assays

For flg22-induced resistance assays, rosette leaves of 4-week-old plants were infiltrated with 1 μ M flg22 or water (mock) for 24 h, before infiltration with *Pst* DC3000 at 10^5 cfu/ml. Inoculated plants were kept in a covered container for 3 days before harvesting the leaves for bacterial quantification. For *Hpa* inoculation, 2-week-old seedlings spray-inoculated with Noco2 strain spores (5×10^4 spores/ml) were incubated at high humidity at 18°C for 6 days until the spores were suspended in water for counting with a hemocytometer. For *Ch* assays, 5 μ l of spores at 2.5×10^5 spores/ml of the IMI 349063A strain grown on Mathur's medium (2.8 g/l glucose, 1.2 g/l $\text{MgSO}_4/7\text{H}_2\text{O}$, 2.7 g/l KH_2PO_4 , 2.2 g/l mycological peptone, 3% Bacto agar) were dropped onto leaves of 4-week-old plants. Inoculated plants were incubated at high humidity for 5 days. The lesion diameter of inoculated leaves was determined with Adobe Photoshop in photo images.

To measure the invasion rates of *Ch* on *Arabidopsis* leaves, 2 μ l of *Ch* spore suspension (5×10^5 spores/ml) was drop-inoculated onto the cotyledons of 10-day-old seedlings. The cotyledons were mounted in water under a coverslip, with the inoculated surface facing the objective lens. The invasion rate (%) was calculated at 3 dpi by the following numerical formula: (the number of conidia with formation of invasive hypha)/(the number of appressoria) \times 100 (Hiruma *et al*, 2011).

Quantitative RT–PCR (qRT–PCR) analysis

Ten-day-old seedlings or 4-week-old plants were treated or syringe-infiltrated with the indicated peptides or bacterial strains and then harvested after the indicated times. Total RNA was isolated from the plant samples using TRI reagent following the manufacturer's instructions (Ambion). Total RNA was reverse-transcribed using an oligo(dT) primer and reverse transcriptase (Roche). Quantitative PCR was performed with the Bio-Rad iQ5 multicolor real-time PCR detection system (Bio-Rad). The expression levels of genes of interest were normalized relative to those of a reference gene, At4 g26410 (Czechowski *et al*, 2005). *PR1*, *NHL10*, and *PDF1.2a* genes were used as defense markers for salicylic acid (SA)-dependent induction, SA-independent induction, and jasmonic acid-/ethylene-dependent induction, respectively (Koornneef *et al*, 2008; Boudsocq *et al*, 2010). Representative results of two or more independent experiments with three biological replicates each are shown, unless otherwise stated.

Microarray analysis

Microarray analysis was performed essentially as described previously (Ross *et al*, 2014), with 10-day-old seedlings (WT, *bak1-3* and *pepr1 pepr2*) exposed to 1 μ M Pep2 for 2 and 10 h.

The hierarchical clustering analysis was conducted on 2,214 genes that exhibited significant changes (more than two-fold, $q < 0.01$) in *bak1-3* plants 10 h after Pep2 application, compared to mock-treated *bak1-3* plants. Based on the expression patterns, these genes were classified into six clusters (Table EV1): Cluster 1 represents genes that are specifically up-regulated in *bak1-3* plants (314 genes); Cluster 2 represents those whose up-regulation was enhanced in *bak1-3* plants (633 genes); Cluster 3 represents those that are equally or less up-regulated in *bak1-3* plants (52 genes); Cluster 4 represents those whose down-regulation was enhanced in *bak1-3* plants (284 genes); Cluster 5 represents those that are equally down-regulated between WT and *bak1-3* plants (66 genes); and Cluster 6 represents those that are specifically down-regulated in *bak1-3* plants (865 genes). The cross-referenced datasets were Exp. ID AT-00391, Exp. ID AT-00113, and Exp. ID AT-00013 in Genevestigator v3, which were also obtained in GeneChip ATH1-121501 Genome Array.

Transient gene expression in *Nicotiana benthamiana*

Agrobacterium tumefaciens GV3101 strains were grown in YEP medium with appropriate antibiotics. Cultures were spun down and resuspended in infiltration buffer (10 mM MgCl_2 , 10 mM MES-KOH pH 5.5) to $\text{OD}_{600} = 0.1$. Suspensions of *Agrobacterium* strains carrying cauliflower mosaic virus (CaMV) 35S promoter (35Spro)::PEPR1-FLAG (pAMPAT) and 35Spro:SERK-HA (pGWB14) (Roux *et al*, 2011) were mixed at a 1:1 ratio and then syringe-infiltrated into 3-week-old *N. benthamiana* leaves. Leaves were harvested 2 days after inoculation.

Protein extraction from plant tissues for immunoblot analysis

Unless otherwise stated, protein extracts were prepared by incubating ground frozen tissues in lysis buffer [50 mM Tris–HCl pH 7.5, 2% SDS, 2 mM DTT, 1 mM AEBSF, 1% (v/v) P9599 protease inhibitor cocktail (Sigma)] for 20 min at room temperature. The supernatants were recovered after centrifugation at 17,000 *g* for 15 min and then subjected to immunoblot analysis with the indicated antibodies.

Co-immunoprecipitation (co-IP) assay

Plant materials were ground in liquid nitrogen and lysed in extraction buffer (50 mM Tris–HCl pH 7.5, 150 mM NaCl, 10% glycerol, 2 mM DTT, 1 mM PMSF (Sigma), 1% (v/v) P9599 protease inhibitor cocktail, 0.5% (v/v) IGEPAL CA-630 (Sigma)). Samples were cleared by centrifugation at 8,000 *g* for 15 min at 4°C and subsequently filtered using a mesh with pore diameter 75 μ m. The supernatants were incubated with anti-Flag M2 antibody (see below) on ice for 10 min and then rotated with protein G beads (Dynabeads, Life Technologies) for 3 h at 4°C. Following three washing steps, the recovered beads were boiled in SDS sample buffer. The eluates were subjected to immunoblot analysis.

Immunoblot analysis

Anti-GFP (B-2), anti-FLAG (M2), anti-HA (3F10), and anti-p44/42 MAPK antibodies were purchased from Santa Cruz Biotechnology,

Sigma, Roche, and Cell Signaling, respectively. Anti-PROPEP3 antibodies raised against both N- and C-terminal fragments of PROPEP3 and anti-Rpn6 antibodies were described previously (Kwok *et al*, 1999; Ross *et al*, 2014). Anti-BAK1 and anti-FLS2 antibodies were generated in rabbits using C-terminal peptides of BAK1 (amino acid residues 600–614, DSTSQIENEYPSGPR) and FLS2 (amino acid residues 1,159–1,173, KANSFREDRNEEDREV) as antigens, respectively, as described previously (Schulze *et al*, 2010).

Molecular weight markers used were Prestained protein marker broad range (Nacalai Tesque in Fig 6C and F), Protein ladder one triple-color (Nacalai Tesque in Fig 6E), and Precision plus protein dual-color standards (Bio-Rad in Figs 4B and 6B). Quantification of immunoblots was performed with ImageJ (<http://rsb.info.nih.gov/ij/>) or CSAnalyzer4 (ATTO). Band intensities were normalized with the values of Ponceau S-stained bands, and then, relative band intensities were calculated with that of the corresponding controls (1.0).

BIK1 phosphorylation assay

Protoplasts were prepared from expanded rosette leaves of 4-week-old *Arabidopsis* plants, according to the previously published method (Yoo *et al*, 2007). 10 µg of the 35Spro:BIK1-HA construct (pAMPAT) was introduced into a 100-µl cell suspension at 2.5×10^5 cells/ml. Six hours after transfection, 1 µM of Pep2 or flg22 was applied for 10 min. Immunoblot analysis for BIK1-HA was conducted as described above for MAPK assay, except that rat anti-HA antibody (3F10, Roche) was used.

Extracellular PROPEP3-Venus detection assay

Five-day-old seedlings grown on MS agar plates under continuous light conditions were transferred to MS liquid medium. Six days later, the medium was replaced either with fresh medium for Pep2 application or with water for bacterial inoculation. One day later, the seedlings were exposed to 1 µM Pep2 for the indicated times, or to the indicated bacterial strains for 20 min. For bacterial inoculation, the inoculated seedlings were washed with water twice and then were further incubated in water for the indicated times. The media were collected and filtered (pore diameter of 0.22 µm) to remove bacteria. Proteins were concentrated from the filtered media with Strataclean resin (Agilent Technologies). After recovery by centrifugation, resins were boiled in SDS sample buffer before separation by SDS-PAGE. Seedling tissues were also subjected to immunoblot analysis.

Salicylate (SA) measurement

SA was extracted from 100 mg plant leaves in 1 ml chloroform/methanol/water (1:2:0.3) containing 160 pmol 2-hydroxybenzoic-3,4,5,6-d₄ acid (SA-d₄; Campro Scientific) as an internal standard and then measured as described previously (Ross *et al*, 2014).

Statistical analysis

The following models were fit to the cycle threshold (C_t) values (for qRT-PCR) or log₂-transformed root length (RL) with the lmer function in the lme4 package or the lm function in the R environment: Ctgr = GTgt+Rr+egtr (Figs 3C and D, 4A, 5A, 7D, EV2F, EV5B, C

and F); Ctgr = Gg+Rr+egtr (Fig EV5G); RLgr = GTgt+Rr+egtr (Fig EV2B and D); and RLgt = GTgt+egtr (Fig EV2C and E), where fixed factors include G, genotype factors; GT, genotype:treatment interactions; T, treatment factors; random factors; R, independent replicate; and e, residual. The mean estimates of the fixed factors were used as the modeled C_t values or RL. Differences between estimated means were compared in two-tailed *t*-tests. For the *t*-tests, the standard errors appropriate for the comparisons were calculated with the variance and covariance values obtained from the model fittings.

Data availability

All microarray data obtained in this study were submitted to Gene Expression Omnibus (Accession GSE40354).

Expanded View for this article is available online.

Acknowledgements

We thank Drs. Xing Wang Deng, Justin Lee, Sacco C. de Vries, Shuhua Yang, Jian-Min Zhou, and Cyril Zipfel for published materials, and Mr. Takaakira Inokuchi for technical support. This work was supported in part by the Max Planck Society, by grants from SFB670 (Y.S.), JST PRESTO (Y.S.), and the Sumitomo Foundation (Y.S.), and by a grant-in-aid for JSPS Fellows (no. 26-4880; K.Y.).

Author contributions

KY and YS conceived the study. KY, MYY, TH, TF, and KH developed and performed the experiments. KY, TH, TF, KT, and KH analyzed the data. KY and YS wrote the manuscript with contribution from the other authors.

Conflict of interest

The authors declare that they have no conflict of interest.

References

- Albrecht C, Russinova E, Kemmerling B, Kwaaitaal M, de Vries SC (2008) Arabidopsis somatic embryogenesis receptor kinase proteins serve brassinosteroid-dependent and -independent signaling pathways. *Plant Physiol* 148: 611–619
- Albrecht C, Boutrot F, Segonzac C, Schwessinger B, Gimenez-Ibanez S, Chinchilla D, Rathjen JP, de Vries SC, Zipfel C (2012) Brassinosteroids inhibit pathogen-associated molecular pattern-triggered immune signaling independent of the receptor kinase BAK1. *Proc Natl Acad Sci USA* 109: 303–308
- Banbury AN, Oakley JD, Sessions RB, Banting G (2003) Tyrphostin A23 inhibits internalization of the transferrin receptor by perturbing the interaction between tyrosine motifs and the medium chain subunit of the AP-2 adaptor complex. *J Biol Chem* 278: 12022–12028
- Belkhadir Y, Nimchuk Z, Hubert DA, Mackey D, Dangl JL (2004) Arabidopsis RIN4 negatively regulates disease resistance mediated by RPS2 and RPM1 downstream or independent of the NDR1 signal modulator and is not required for the virulence functions of bacterial type III effectors AvrRpt2 or AvrRpm1. *Plant Cell* 16: 2822–2835
- Belkhadir Y, Jaillais Y, Eppe P, Balsemão-Pires E, Dangl JL, Chory J (2012) Brassinosteroids modulate the efficiency of plant immune responses to microbe-associated molecular patterns. *Proc Natl Acad Sci USA* 109: 297–302

- Boller T, Felix G (2009) A renaissance of elicitors: perception of microbe-associated molecular patterns and danger signals by pattern-recognition receptors. *Annu Rev Plant Biol* 60: 379–406
- Boudsocq M, Willmann MR, McCormack M, Lee H, Shan L, He P, Bush J, Cheng S-H, Sheen J (2010) Differential innate immune signalling via Ca^{2+} sensor protein kinases. *Nature* 464: 418–U116
- Cheng W, Munkvold KR, Gao H, Mathieu J, Schwizer S, Wang S, Yan Y-B, Wang J, Martin GB, Chai J (2011) Structural analysis of *Pseudomonas syringae* AvrPtoB bound to host BAK1 reveals two similar kinase-interacting domains in a type III effector. *Cell Host Microbe* 10: 616–626
- Chinchilla D, Zipfel C, Robatzek S, Kemmerling B, Nürnberger T, Jones JD, Felix G, Boller T (2007) A flagellin-induced complex of the receptor FLS2 and BAK1 initiates plant defence. *Nature* 448: 497–500
- Cui H, Tsuda K, Parker JE (2015) Effector-triggered immunity: from pathogen perception to robust defense. *Annu Rev Plant Biol* 66: 487–511.
- Czechowski T, Stitt M, Altmann T, Udvardi MK, Scheible WR (2005) Genome-wide identification and testing of superior reference genes for transcript normalization in *Arabidopsis*. *Plant Physiol* 139: 5–17
- Debener T, Lehnackers H, Arnold M, Dangl JL (1991) Identification and molecular mapping of a single *Arabidopsis thaliana* locus determining resistance to a phytopathogenic *Pseudomonas-syringae* isolate. *Plant J* 1: 289–302
- Dong X, Mindrinos M, Davis KR, Ausubel FM (1991) Induction of *Arabidopsis* defense genes by virulent and avirulent *Pseudomonas syringae* strains and by a cloned avirulence gene. *Plant Cell* 3: 61–72
- Emans N, Zimmermann S, Fischer R (2002) Uptake of a fluorescent marker in plant cells is sensitive to brefeldin A and wortmannin. *Plant Cell* 14: 71–86
- Flury P, Klausner D, Schulze B, Boller T, Bartels S (2013) The anticipation of danger: microbe-associated molecular pattern perception enhances AtPep-triggered oxidative burst. *Plant Physiol* 161: 2023–2035
- Gao M, Wang X, Wang D, Xu F, Ding X, Zhang Z, Bi D, Cheng YT, Chen S, Li X, Zhang Y (2009) Regulation of cell death and innate immunity by two receptor-like kinases in *Arabidopsis*. *Cell Host Microbe* 6: 34–44
- Goehre V, Spallek T, Haeweker H, Mersmann S, Mentzel T, Boller T, de Torres M, Mansfield JW, Robatzek S (2008) Plant pattern-recognition receptor FLS2 is directed for degradation by the bacterial ubiquitin ligase AvrPtoB. *Curr Biol* 18: 1824–1832
- Gust AA, Felix G (2014) Receptor like proteins associate with SOBIR1-type of adaptors to form bimolecular receptor kinases. *Curr Opin Plant Biol* 21: 104–111
- Halter T, Imkamp J, Mazzotta S, Wierzbica M, Postel S, Bücherl C, Kiefer C, Stahl M, Chinchilla D, Wang X, Nürnberger T, Zipfel C, Clouse S, Borst JW, Boeren S, de Vries SC, Tax F, Kemmerling B (2014) The leucine-rich repeat receptor kinase BIR2 is a negative regulator of BAK1 in plant immunity. *Curr Biol* 24: 134–143
- He K, Gou X, Yuan T, Lin H, Asami T, Yoshida S, Russell SD, Li J (2007) BAK1 and BKK1 regulate brassinosteroid-dependent growth and brassinosteroid-independent cell-death pathways. *Curr Biol* 17: 1109–1115
- Heese A, Hann DR, Gimenez-Ibanez S, Jones AM, He K, Li J, Schroeder JI, Peck SC, Rathjen JP (2007) The receptor-like kinase SERK3/BAK1 is a central regulator of innate immunity in plants. *Proc Natl Acad Sci USA* 104: 12217–12222
- Hiruma K, Nishiuchi T, Kato T, Bednarek P, Okuno T, Schulze-Lefert P, Takano Y (2011) *Arabidopsis* enhanced disease resistance 1 is required for pathogen-induced expression of plant defensins in nonhost resistance, and acts through interference of MYC2-mediated repressor function. *Plant J* 67: 980–992
- Huffaker A, Pearce G, Ryan CA (2006) An endogenous peptide signal in *Arabidopsis* activates components of the innate immune response. *Proc Natl Acad Sci USA* 103: 10098–10103
- Jones JD, Dangl JL (2006) The plant immune system. *Nature* 444: 323–329
- Kadota Y, Sklenar J, Derbyshire P, Strandsfeld L, Asai S, Ntoukakis V, Jones JD, Shirasu K, Menke F, Jones A, Zipfel C (2014) Direct regulation of the NADPH oxidase RBOHD by the PRR-associated kinase BIK1 during plant immunity. *Mol Cell* 54: 43–55
- Kemmerling B, Schwedt A, Rodríguez P, Mazzotta S, Frank M, Qamar SA, Mengiste T, Betsuyaku S, Parker JE, Müssig C, Thomma BP, Albrecht C, de Vries SC, Hirt H, Nürnberger T (2007) The BRI1-associated kinase 1, BAK1, has a brassinolide-independent role in plant cell-death control. *Curr Biol* 17: 1116–1122
- Kim HS, Desveaux D, Singer AU, Patel P, Sondek J, Dangl JL (2005a) The *Pseudomonas syringae* effector AvrRpt2 cleaves its C-terminally acylated target, RIN4, from *Arabidopsis* membranes to block RPM1 activation. *Proc Natl Acad Sci USA* 102: 6496–6501
- Kim MG, da Cunha L, McFall AJ, Belkadir Y, DebRoy S, Dangl JL, Mackey D (2005b) Two *Pseudomonas syringae* type III effectors inhibit RIN4-regulated basal defense in *Arabidopsis*. *Cell* 121: 749–759
- Koornneef A, Leon-Reyes A, Ritsema T, Verhage A, Den Otter FC, Van Loon LC, Pieterse CMJ (2008) Kinetics of salicylate-mediated suppression of jasmonate signaling reveal a role for redox modulation. *Plant Physiol* 147: 1358–1368
- Krasileva KV, Zheng C, Leonelli L, Goritschnig S, Dahlbeck D, Staskiewicz BJ (2011) Global analysis of *Arabidopsis*/downy mildew interactions reveals prevalence of incomplete resistance and rapid evolution of pathogen recognition. *PLoS ONE* 6: e28765
- Krol E, Mentzel T, Chinchilla D, Boller T, Felix G, Kemmerling B, Postel S, Arents M, Jeworutzki E, Al-Rasheid KA, Becker D, Hedrich R (2010) Perception of the *Arabidopsis* danger signal peptide 1 involves the pattern recognition receptor AtPEPR1 and its close homologue AtPEPR2. *J Biol Chem* 285: 13471–13479
- Kwok SF, Staub JM, Deng XW (1999) Characterization of two subunits of *Arabidopsis* 19S proteasome regulatory complex and its possible interaction with the COP9 complex. *J Mol Biol* 285: 85–95
- Laluk K, Luo H, Chai M, Dhawan R, Lai Z, Mengiste T (2011) Biochemical and genetic requirements for function of the immune response regulator BOTRYTIS-INDUCED KINASE1 in plant growth, ethylene signaling, and PAMP-triggered immunity in *Arabidopsis*. *Plant Cell* 23: 2831–2849
- Li J, Wen J, Lease KA, Doke JT, Tax FE, Walker JC (2002) BAK1, an *Arabidopsis* LRR receptor-like protein kinase, interacts with BRI1 and modulates brassinosteroid signaling. *Cell* 110: 213–222
- Li M, Ma X, Chiang YH, Yadeta KA, Ding P, Dong L, Zhao Y, Li X, Yu Y, Zhang L, Shen QH, Xia B, Coaker G, Liu D, Zhou JM (2014) Proline isomerization of the immune receptor-interacting protein RIN4 by a cyclophilin inhibits effector-triggered immunity in *Arabidopsis*. *Cell Host Microbe* 16: 473–483
- Liebrand TWH, van den Burg HA, Joosten MHAJ (2014) Two for all: receptor-associated kinases SOBIR1 and BAK1. *Trends Plant Sci* 19: 123–132
- Lin W, Lu D, Gao X, Jiang S, Ma X, Wang Z, Mengiste T, He P, Shan L (2013) Inverse modulation of plant immune and brassinosteroid signaling pathways by the receptor-like cytoplasmic kinase BIK1. *Proc Natl Acad Sci USA* 110: 12114–12119
- Lin W, Li B, Lu D, Chen S, Zhu N, He P, Shan L (2014) Tyrosine phosphorylation of protein kinase complex BAK1/BIK1 mediates *Arabidopsis* innate immunity. *Proc Natl Acad Sci USA* 111: 3632–3637

- Liu Z, Wu Y, Yang F, Zhang Y, Chen S, Xie Q, Tian X, Zhou JM (2013) BIK1 interacts with PEPs to mediate ethylene-induced immunity. *Proc Natl Acad Sci USA* 110: 6205–6210
- Lu D, Wu S, Gao X, Zhang Y, Shan L, He P (2010) A receptor-like cytoplasmic kinase, BIK1, associates with a flagellin receptor complex to initiate plant innate immunity. *Proc Natl Acad Sci USA* 107: 496–501
- Lu D, Lin W, Gao X, Wu S, Cheng C, Avila J, Heese A, Devarenne TP, He P, Shan L (2011) Direct ubiquitination of pattern recognition receptor FLS2 attenuates plant innate immunity. *Science* 332: 1439–1442
- Ma Y, Walker RK, Zhao Y, Berkowitz GA (2012) Linking ligand perception by PEP pattern recognition receptors to cytosolic Ca^{2+} elevation and downstream immune signaling in plants. *Proc Natl Acad Sci USA* 109: 19852–19857
- Macho AP, Schwessinger B, Ntoukakis V, Brutus A, Segonzac C, Roy S, Kadota Y, Oh M-H, Sklenar J, Derbyshire P, Lozano-Duran R, Malinovskiy FG, Monaghan J, Menke FL, Huber SC, He SY, Zipfel C (2014) A bacterial tyrosine phosphatase inhibits plant pattern recognition receptor activation. *Science* 343: 1509–1512
- Macho AP, Zipfel C (2014) Plant PRRs and the activation of innate immune signaling. *Mol Cell* 54: 263–272
- Macho AP, Zipfel C (2015) Targeting of plant pattern recognition receptor-triggered immunity by bacterial type-III secretion system effectors. *Curr Opin Microbiol* 23: 14–22
- Nam KH, Li J (2002) BRI1/BAK1, a receptor kinase pair mediating brassinosteroid signaling. *Cell* 110: 203–212
- Nicaise V, Joe A, Jeong B-R, Korneli C, Boutrot F, Westedt I, Staiger D, Alfano JR, Zipfel C (2013) *Pseudomonas* HopU1 modulates plant immune receptor levels by blocking the interaction of their mRNAs with GRP7. *EMBO J* 32: 701–712
- Nishimura MT, Stein M, Hou BH, Vogel JP, Edwards H, Somerville SC (2003) Loss of a callose synthase results in salicylic acid-dependent disease resistance. *Science* 301: 969–972
- O'Connell R, Herbert C, Sreenivasaprasad S, Khatib M, Esquerre-Tugay MT, Dumas B (2004) A novel *Arabidopsis-Colletotrichum pathosystem* for the molecular dissection of plant-fungal interactions. *Mol Plant Microbe Interact* 17: 272–282
- Parker JE, Szabo V, Staskawicz BJ, Lister C, Dean C, Daniels MJ, Jones JGD (1993) Phenotypic characterization and molecular mapping of the *Arabidopsis-thaliana* locus RPP5, determining disease resistance to *Peronospora-parasitica*. *Plant J* 4: 821–831
- Ranf S, Grimmer J, Poeschl Y, Pecher P, Chinchilla D, Scheel D, Lee J (2012) Defense-related calcium signaling mutants uncovered via a quantitative high-throughput screen in *Arabidopsis thaliana*. *Mol Plant* 5: 115–130
- Robatzek S, Chinchilla D, Boller T (2006) Ligand-induced endocytosis of the pattern recognition receptor FLS2 in *Arabidopsis*. *Genes Dev* 20: 537–542
- Rock KL, Gramm C, Rothstein L, Clark K, Stein R, Dick L, Hwang D, Goldberg AL (1994) Inhibitors of the proteasome block the degradation of most cell proteins and the generation of peptides presented on MHC class I molecules. *Cell* 78: 761–771
- Ronald PC, Beutler B (2010) Plant and animal sensors of conserved microbial signatures. *Science* 330: 1061–1064
- Ross A, Yamada K, Hiruma K, Yamashita-Yamada M, Lu X, Takano Y, Tsuda K, Saijo Y (2014) The *Arabidopsis* PEP pathway couples local and systemic plant immunity. *EMBO J* 33: 62–75
- Roux M, Schwessinger B, Albrecht C, Chinchilla D, Jones A, Holton N, Malinovskiy FG, Tör M, de Vries S, Zipfel C (2011) The *Arabidopsis* leucine-rich repeat receptor-like kinases BAK1/SERK3 and BKK1/SERK4 are required for innate immunity to hemibiotrophic and biotrophic pathogens. *Plant Cell* 23: 2440–2455
- Roux ME, Rasmussen MW, Palma K, Lolte S, Regué AM, Bethke G, Glazebrook J, Zhang W, Sieburth L, Larsen MR, Mundy J, Petersen M (2015) The mRNA decay factor PAT1 functions in a pathway including MAP kinase 4 and immune receptor SUMM2. *EMBO J* 34: 593–608
- Rustérucci C, Aviv DH, Holt BF, Dangl JL, Parker JE (2001) The disease resistance signaling components EDS1 and PAD4 are essential regulators of the cell death pathway controlled by LSD1 in *Arabidopsis*. *Plant Cell* 13: 2211–2224
- Saijo Y (2010) ER quality control of immune receptors and regulators in plants. *Cell Microbiol* 12: 716–724
- Schulze B, Mentzel T, Jehle AK, Mueller K, Beeler S, Boller T, Felix G, Chinchilla D (2010) Rapid heteromerization and phosphorylation of ligand-activated plant transmembrane receptors and their associated kinase BAK1. *J Biol Chem* 285: 9444–9451
- Schwessinger B, Roux M, Kadota Y, Ntoukakis V, Sklenar J, Jones A, Zipfel C (2011) Phosphorylation-dependent differential regulation of plant growth, cell death, and innate immunity by the regulatory receptor-like kinase BAK1. *PLoS Genet* 7: e1002046
- Segonzac C, Macho AP, Sanmartin M, Ntoukakis V, Sanchez-Serrano JJ, Zipfel C (2014) Negative control of BAK1 by protein phosphatase 2A during plant innate immunity. *EMBO J* 33: 2069–2079
- Shan L, He P, Li J, Heese A, Peck SC, Nürnberger T, Martin GB, Sheen J (2008) Bacterial effectors target the common signaling partner BAK1 to disrupt multiple MAMP receptor-signaling complexes and impede plant immunity. *Cell Host Microbe* 4: 17–27
- Shao F, Golstein C, Ade J, Stoutemyer M, Dixon JE, Innes RW (2003) Cleavage of *Arabidopsis* PBS1 by a bacterial type III effector. *Science* 301: 1230–1233
- Smith JM, Salamango DJ, Leslie ME, Collins CA, Heese A (2014) Sensitivity to Flg22 is modulated by ligand-induced degradation and *de novo* synthesis of the endogenous flagellin-receptor flagellin-sensing2. *Plant Physiol* 164: 440–454
- Stuart LM, Paquette N, Boyer L (2013) Effector-triggered versus pattern-triggered immunity: how animals sense pathogens. *Nature Rev Immunol* 13: 199–206
- Sun YD, Li L, Macho AP, Han ZF, Hu ZH, Zipfel C, Zhou JM, Chai JJ (2013) Structural basis for flg22-induced activation of the *Arabidopsis* FLS2-BAK1 immune complex. *Science* 342: 624–628
- Sun T, Zhang Q, Gao M, Zhang Y (2014) Regulation of SOBIR1 accumulation and activation of defense responses in bir1-1 by specific components of ER quality control. *Plant J* 77: 748–756
- Tintor N, Ross A, Kanehara K, Yamada K, Fan L, Kemmerling B, Nürnberger T, Tsuda K, Saijo Y (2013) Layered pattern receptor signaling via ethylene and endogenous elicitor peptides during *Arabidopsis* immunity to bacterial infection. *Proc Natl Acad Sci USA* 110: 6211–6216
- Wang Z, Meng P, Zhang X, Ren D, Yang S (2011) BON1 interacts with the protein kinases BIR1 and BAK1 in modulation of temperature-dependent plant growth and cell death in *Arabidopsis*. *Plant J* 67: 1081–1093
- Wildermuth MC, Dewdney J, Wu G, Ausubel FM (2001) Isochorismate synthase is required to synthesize salicylic acid for plant defence. *Nature* 414: 562–565
- Willmann R, Lajunen HM, Erbs G, Newman MA, Kolb D, Tsuda K, Katagiri F, Fliegmann J, Bono JJ, Cullimore JV, Jehle AK, Götz F, Kulik A, Molinaro A, Lipka V, Gust AA, Nürnberger T (2011) *Arabidopsis* lysin-motif proteins LYM1 LYM3 CERK1 mediate bacterial peptidoglycan sensing and immunity to bacterial infection. *Proc Natl Acad Sci USA* 108: 19824–19829

- Xiang TT, Zong N, Zou Y, Wu Y, Zhang J, Xing WM, Li Y, Tang XY, Zhu LH, Chai JJ, Zhou JM (2008) *Pseudomonas syringae* effector AvrPto blocks innate immunity by targeting receptor kinases. *Curr Biol* 18: 74–80
- Xiang TT, Zong N, Zhang J, Chen JF, Chen MS, Zhou JM (2011) BAK1 is not a target of the *Pseudomonas syringae* effector AvrPto. *Mol Plant Microbe Interact* 24: 100–107
- Xin X-F, He SY (2013) *Pseudomonas syringae* pv. tomato DC3000: a model pathogen for probing disease susceptibility and hormone signaling in plants. *Annu Rev Phytopathol* 51: 473–498
- Yamaguchi Y, Pearce G, Ryan CA (2006) The cell surface leucine-rich repeat receptor for AtPep1, an endogenous peptide elicitor in *Arabidopsis*, is functional in transgenic tobacco cells. *Proc Natl Acad Sci USA* 103: 10104–10109
- Yamaguchi Y, Huffaker A, Bryan AC, Tax FE, Ryan CA (2010) PEPR2 is a second receptor for the Pep1 and Pep2 peptides and contributes to defense responses in *Arabidopsis*. *Plant Cell* 22: 508–522
- Yamaguchi Y, Huffaker A (2011) Endogenous peptide elicitors in higher plants. *Curr Opin Plant Biol* 14: 351–357
- Yang S, Yang H, Grisafi P, Sanchatjate S, Fink GR, Sun Q, Hua J (2006) The *BON/CPN* gene family represses cell death and promotes cell growth in *Arabidopsis*. *Plant J* 45: 166–179
- Yoo SD, Cho YH, Sheen J (2007) *Arabidopsis* mesophyll protoplasts: a versatile cell system for transient gene expression analysis. *Nat Protoc* 2: 1565–1572
- Yuan J, He SY (1996) The *Pseudomonas syringae* Hrp regulation and secretion system controls the production and secretion of multiple extracellular proteins. *J Bacteriol* 178: 6399–6402
- Zeng W, He SY (2010) A prominent role of the flagellin receptor flagellin-sensing2 in mediating stomatal response to *Pseudomonas syringae* pv tomato DC3000 in *Arabidopsis*. *Plant Physiol* 153: 1188–1198
- Zhang J, Li W, Xiang T, Liu Z, Laluk K, Ding X, Zou Y, Gao M, Zhang X, Chen S, Mengiste T, Zhang Y, Zhou JM (2010) Receptor-like cytoplasmic kinases integrate signaling from multiple plant immune receptors and are targeted by a *Pseudomonas syringae* effector. *Cell Host Microbe* 7: 290–301
- Zhang Z, Wu Y, Gao M, Zhang J, Kong Q, Liu Y, Ba H, Zhou J, Zhang Y (2012) Disruption of PAMP-induced MAP kinase cascade by a *Pseudomonas syringae* effector activates plant immunity mediated by the NB-LRR protein SUMM2. *Cell Host Microbe* 11: 253–263
- Zhang Q, Sun T, Zhang Y (2015) ER quality control components UGGT and STT3a are required for activation of defense responses in Bir1-1. *PLoS ONE* 10: e0120245
- Zipfel C, Robatzek S, Navarro L, Oakeley EJ, Jones JD, Felix G, Boller T (2004) Bacterial disease resistance in *Arabidopsis* through flagellin perception. *Nature* 428: 764–767
- Zipfel C, Kunze G, Chinchilla D, Caniard A, Jones JD, Boller T, Felix G (2006) Perception of the bacterial PAMP EF-Tu by the receptor EFR restricts *Agrobacterium*-mediated transformation. *Cell* 125: 749–760